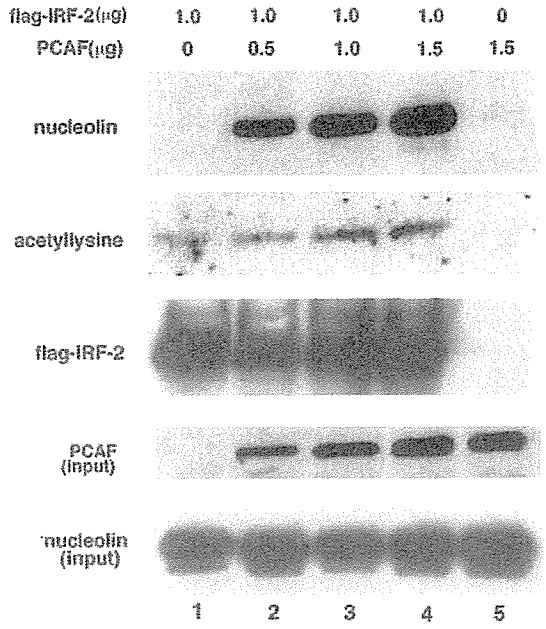

Figure 5 Interferon regulatory factor-2 (IRF-2) associates nucleolin in the presence of p300/CBP-associated factor (PCAF). 293T cells were transfected with several indicated amount of PCAF (lanes 1–5) and flag-IRF-2 (1 μg) (lanes 1–4). Cell lysate were incubated with anti-flag M2 agarose and flag-peptide eluted fraction were immunoblotted with anti-nucleolin, anti-acetyllysine and anti-flag antibodies. Whole cell lysate of transfected cells were immunoblot with anti-PCAF and anti-nucleolin antibodies.

We examined the localization of IRF-2 and nucleolin. HeLa cells transfected with flag-IRF-2 or a mutant flag-IRF-2K75R partially defective in acetylation (Masumi *et al*, 2003) with or without PCAF were fixed with paraformaldehyde and immunostained with an anti-flag antibody conjugated to cy3, and then an anti-nucleolin antibody linked with fluorescein isothiocyanate (FITC). Immunostained cells were visualized by laser scanning confocal microscopy. As shown in Figure 6a, there was no significant difference between wild-type IRF-2 and IRF-2K75R mutant-transfected HeLa cells, with nucleolin localized mainly in the nucleolus and to a lesser extent in the nucleus. Although IRF-2 localized predominantly in the nucleus, some was also localized in nucleolus. We observed that IRF-2 colocalized with nucleolin in a peri-nucleolar location. p300/CBP-associated factor transfection with both wild-type IRF-2 and K75R mutant did not change the colocalization of IRF-2 and nucleolin significantly.

To confirm if acetylatable IRF-2 recruits to nucleolin, a protein–protein interaction assay was performed using IRF-2 stably transfected cells. Cell lysates were prepared from HeLa and K562 cells stably transfected with flag-tagged wild-type IRF-2 or IRF-2K75R (Masumi *et al*., 2003). Lysates were incubated with anti-flag M2-agarose, and the precipitates were subjected to Western blot analysis using an anti-nucleolin antibody. In both HeLa and K562 cells, appreciable amounts of PCAF and p300 were detected (data not shown). As shown in Figure 6b, nucleolin–IRF-2 interaction was observed in both HeLa and K562 cells that expressed wild-type IRF-2. However, in cells that expressed the K75RIRF-2 mutant (Masumi *et al*., 2003), the nucleolin interaction was markedly diminished. These results suggest that IRF-2 is acetylated by histone acetylases such as PCAF and p300 in these cells, and that acetylated IRF-2 preferentially associates with nucleolin.

Nucleolin transactivates interferon regulatory factor-2-enhanced H4 promoter activity

Interferon regulatory factor-2 functions as an activator for the H4 gene promoter in NIH3T3 cells (Masumi *et al*., 2003). To examine the functional role for nucleolin in IRF-2-dependent transcription, an *H4* gene reporter plasmid was transfected into NIH3T3 cells with IRF-2, PCAF and nucleolin. As shown in Figure 7a, transfection of nucleolin and PCAF both increased IRF-2-induced *H4* promoter activation. Co-transfection of nucleolin with PCAF further enhanced IRF-2-induced *H4* promoter activity (Figure 7a). In NIH3T3 cells, endogenous p300 may also induce IRF-2-dependent transactivation through acetylation, resulting in its interaction with nucleolin. In addition, co-transfection with HAT-deficient PCAF had no effect on nucleolin/IRF-2 activity. (Figure 7a). Co-transfection of the K75RIRF-2 mutant with PCAF/nucleolin resulted in a much lower activation of the *H4* promoter in NIH3T3 cells than with wild-type IRF-2 (Figure 7b). To examine nucleolin contribution to IRF-2-mediated *H4* promoter activation, we performed luciferase reporter assay using nucleolin small interfering RNA (siRNA). NIH3T3 cells were transfected with nucleolin siRNA to knock-down endogenous nucleolin and then transfected with IRF-2, PCAF with *H4* promoter-conjugated luciferase reporter. Compared to the control siRNA transfection, nucleolin siRNA transfection reduced the endogenous nucleolin protein in NIH3T3 cells (Figure 7d) and downregulated the IRF-2/PCAF-mediated *H4* promoter activation (Figure 7c). These results confirm that nucleolin contributes to IRF-2/PCAF-mediated transcriptional activation in NIH3T3 cells.

We have shown previously that acetylation of IRF-2 is related to cell growth (Masumi *et al*., 2003) and have therefore investigated whether IRF-2 is associated with nucleolin in growing NIH3T3 cells. For confocal analysis, we detected that IRF-2 and nucleolin were localized in nuclei and nucleoli in both growing and growth-arrested NIH3T3 cells. There was no significant difference between either type of NIH3T3 cell (Figure 8a). We performed a DNA affinity binding assay with biotinylated *H4* promoter oligonucleotides that had been conjugated to magnetic beads. Nuclear extracts from growing and growth-arrested cells were incubated with the beads-conjugated *H4* promoter DNA. Interferon regulatory factor-2 was detected in an eluted fraction from beads incubated with growing cell nuclear extract as reported earlier (Figure 8b) (Masumi *et al*., 2003). We found that while a similar level of nucleolin was detected in both growing and growth-arrested cells, H4 promoter DNA was bound to

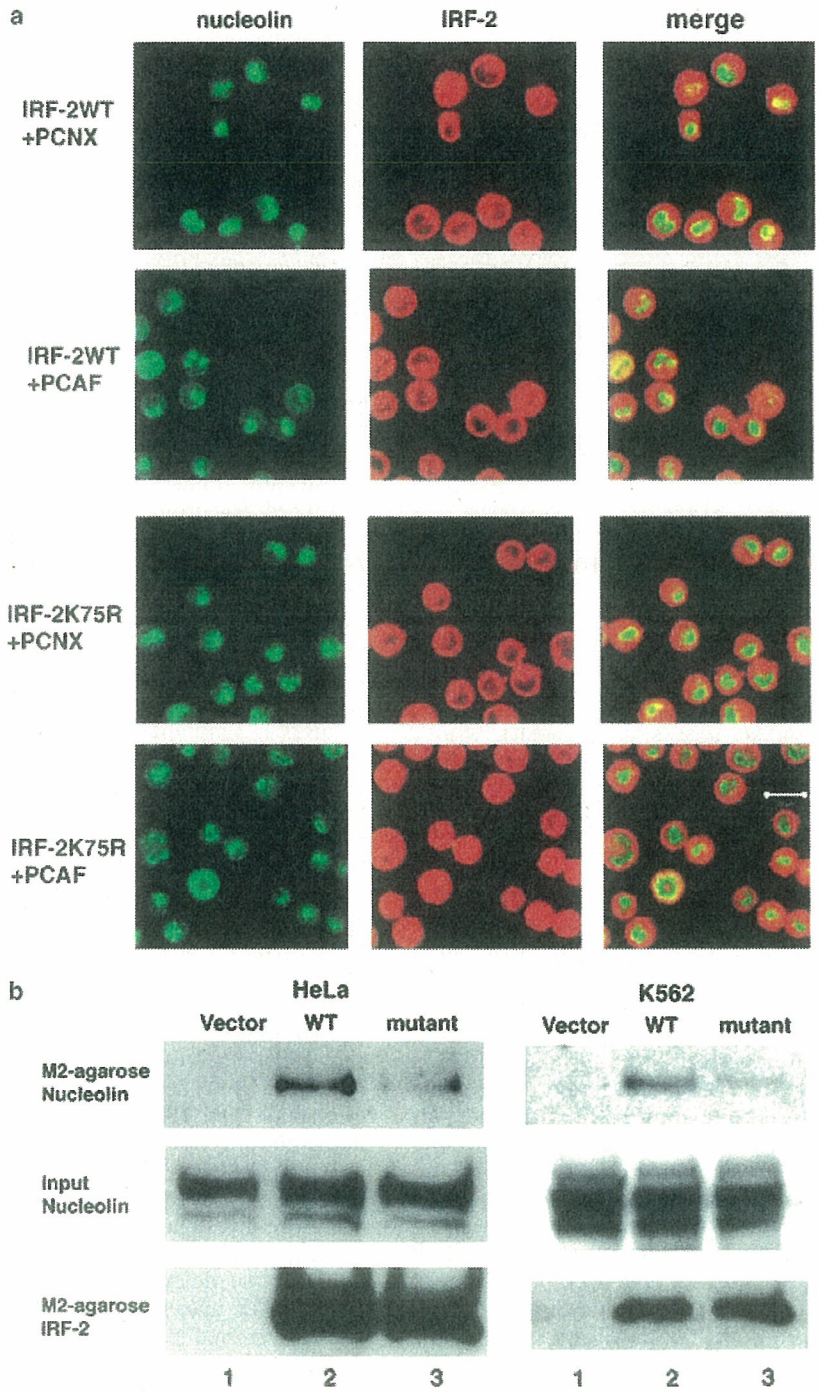

Figure 6 Interferon regulatory factor-2 (IRF-2) colocalizes and associates with nucleolin. (**a**) Laser scanning confocal microscopy was carried out on HeLa cells transiently transfected with flag-IRF-2 and flag-IRF-2K75R with or without p300/CBP-associated factor (PCAF). The cells were fixed with paraformaldehyde 24 h after transfection and lysed with 0.2% TritonX-100 for 10 min. Then, cells were immunocytostained with a anti-flag conjugated to Cy3 (red fluorescence) antibody for 24 h, following which, washed cells were immunostained with anti-nucleolin linked with fluorescein isothiocyanate (FITC) (green fluorescence) for 24 h. These washed cells were covered with glycerol and examined by laser scanning confocal microscopy. Colocalization of proteins results in a merging of red and green fluorescence to produce a yellow image. (**b**) Cell lysate from HeLa (left) and K562 (right) cells stably transfected with an empty vector (lane 1), flag-IRF-2 (lane 2) and flag-IRF-2K75R mutant (lane 3) were incubated with anti-flag M2-agarose and flag-peptide-eluted fractions were separated on SDS–10% PAGE and immunoblotted with anti-nucleolin (top) and anti-IRF-2 (bottom) antibodies. Whole cell lysates were separated on SDS–10% PAGE and immunoblotted with an anti-nucleolin antibody (middle).

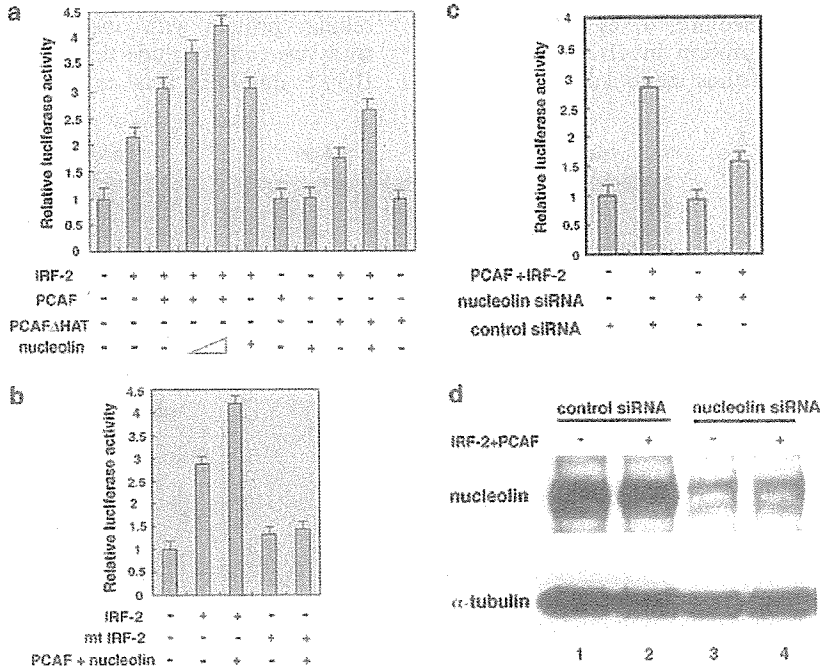

Figure 7 Nucleolin activates interferon regulatory factor-2 (IRF-2)-dependent *H4* promoter activity. (**a**) *H4* promoter reporter (400 ng), nucleolin (100 and 200 ng), p300/CBP-associated factor (PCAF)PCNX (100 and 200 ng) and PCAFΔhistone acetyl transferase (HAT)PCNX (200 ng) were transfected with IRF-2pcDNA3.1 (20 ng) into NIH3T3 cells. Luciferase activity was analysed 48 h after transfection. (**b**) Wild-type IRF-2 or mutant IRF-2 (IRF-2K75R) was transfected with nucleolin/PCAF with the *H4* promoter reporter as described in (**a**). Luciferase activity was analysed 48 h after transfection. The mean ± s.d. from three separate experiments were calculated after normalization with TK Renilla activity. (**c**) Nucleolin small interfering RNA (siRNA) abrogates IRF-2/PCAF-induced *H4* promoter activation. Nucleolin siRNA was transfected into NIH3T3 cells and then PCAFPCNX and IRF-2pcDNA3.1 were transfected into NIH3T3 cells with *H4* promoter reporter. At 24 h after transfection of plasmids, luciferase activity was analysed. (**d**) Immunoblot analysis of NIH3T3 cell lysate transfected with nucleolin siRNA and plasmids as described in (**c**) using anti-nucleolin and anti-α-tubulin antibodies.

the nucleolin from growing cells only (Figure 8b). These finding are consistent with previous results, which support that the interaction of nucleolin and acetylated IRF-2 in growing cells mediate *H4* gene promoter activity (Masumi *et al*., 2003).

From these results, it appears that the acetylation of IRF-2 rather than the change of colocalization of both factors is important for the interaction of IRF-2 and nucleolin in growing NIH3T3 cells. To confirm the association of nucleolin with IRF-2 on the *H4* promoter, chromatin immunoprecipitation analysis was performed. Chromatin was isolated from NIH3T3 cells transfected with PCAFPCNX and immunoprecipitated with anti-IRF-2 and anti-nucleolin and anti-PCAF antibodies. Immunoprecipitates were performed with polymerase chain reaction (PCR) using *H4* promoter primer as described earlier (Masumi *et al*., 2003). As shown in Figure 8c, PCAF transfection slightly enhance the PCAF binding to *H4* promoter, however, a greater amount of nucleolin was bound to the *H4* promoter in the PCAF-transfected cells compared to control cells. In addition, a greater amount of IRF-2 was also bound to the *H4* promoter in PCAF-transfected cells compared to non-transfected cells. From these results it appears that, in NIH3T3 cells, IRF-2 and nucleolin bound the *H4* promoter more tightly following transfection with exogenous PCAF. We conclude that nucleolin binds to acetylated IRF-2 and IRF-2/PCAF/nucleolin complexes in turn stimulate the activation of gene transcription, which drives cell growth (Figure 9).

Discussion

In this study, we have demonstrated that nucleolin acts as a positive modulator of IRF-2-dependent transcriptional activation through an association with IRF-2. Nucleolin is one of the most abundant nucleolar proteins in rapidly growing eukaryotic cells. It is multifunctional and thought to be involved in many cellular processes, including ribosome biogenesis, the processing of ribosomal RNA, mRNA stability, transcriptional regulation and cell proliferation, and it is also a downstream target of several signal transduction pathways (Ginisty *et al*., 1992; Srivastava and Pollard, 1999). Nucleolin has been shown by proteomic analysis to associate with various proteins, such as B23, Ku80, eIF2a and the RNA binding proteins (RNP) complex (Yanagida *et al*., 2001). Ying *et al*. (2000) reported that the interaction of nucleolin with Myb downregulated Myb transcriptional activity. Recently, Grinstein *et al*.

(2002) reported that nucleolin is a key activator of the HPV18 oncogene transcription involved in chromatin structure regulation and thus identified nuclelolin as a cellular protein with oncogenic potential. From our study we can conclude that for *H4* gene regulation by IRF-2, nucleolin acts as an oncogenic activator via

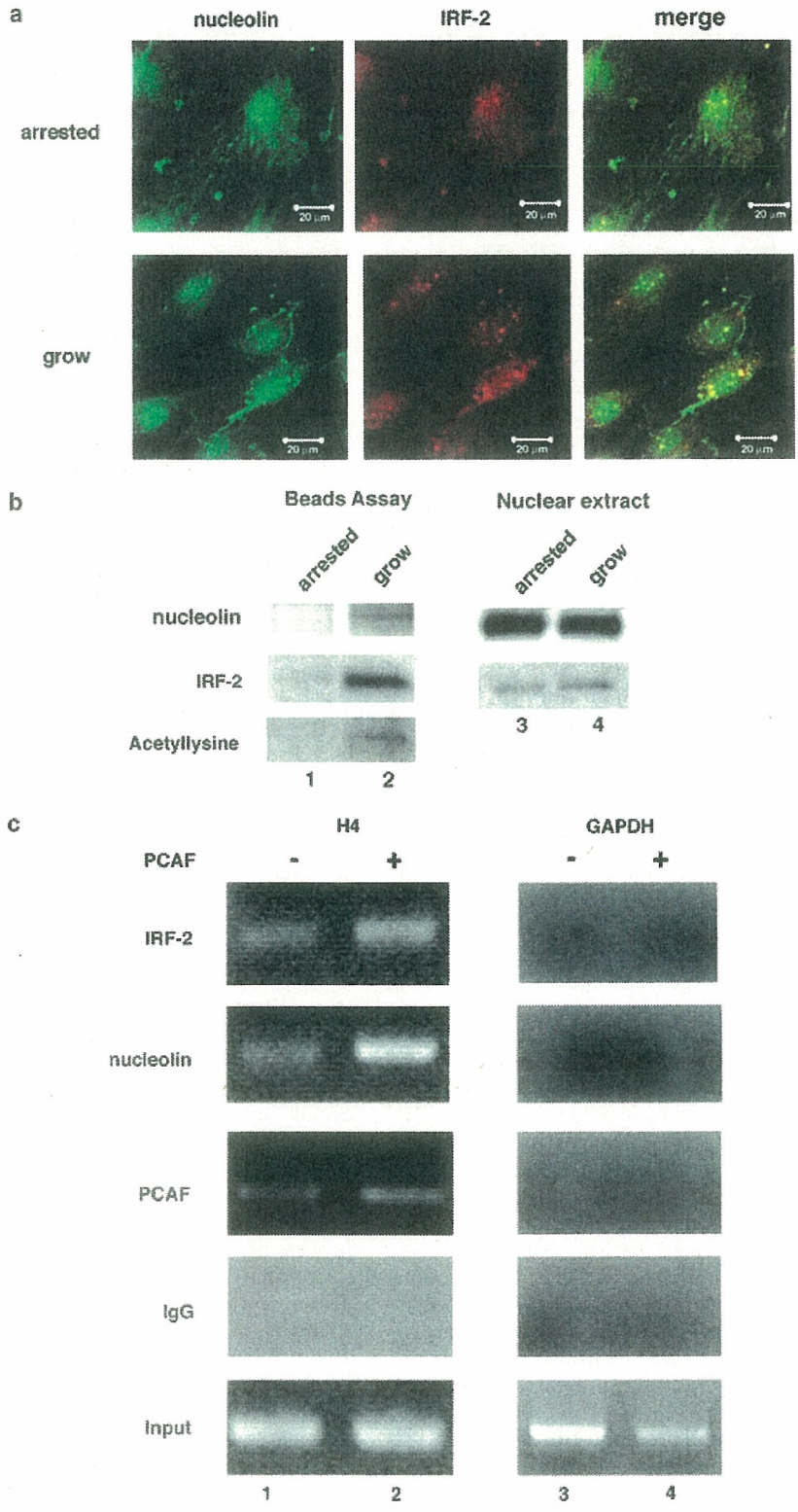

transcriptional activation, suggesting an involvement in cell growth regulation.

Previously, we demonstrated in NIH3T3 cells that lysine residues 75 and 78 in the IRF-2 DNA-binding domain are the major acetylation sites and that the IRF-2K75R mutant showed reduced *H4* promoter activity. As reported in our previous paper, p300 acts as the main acetylase for IRF-2 in NIH3T3 cells because the level of PCAF expression is so very low. However, exogenous PCAF transfection induced IRF-2-dependent transcriptional activation (Masumi *et al*., 1999), and exogenous PCAF might induce IRF-2 acetylation in NIH3T3 cells. We also found that transfection with another histone acetylase GCN5 induced IRF-2 acetylation (data not shown) and nucleolin-IRF-2 interaction in 293T cells. We previously concluded that in NIH3T3 cells acetylated IRF-2 binds to the *H4* promoter with p300 to regulate the H4 gene (Masumi *et al*., 2003). However, in cells with a high amount of PCAF or GCN5, IRF-2 may be acetylated by both histone acetyltransferases, as well as p300, recruit nucleolin and thus regulate specific promoters. In the *H4* promoter assay, we demonstrated that PCAF acetyltransferase activity was required for efficient activation of transcription mediated by IRF-2/nucleolin. Interferon regulatory factor-2K75R mutant partially defective acetylation reduces the activation of the *H4* promoter in the presence of PCAF/nucleolin, consistent with the results of the poor association of IRF-2K75R with nucleolin in stable transfectants.

We observed that in HeLa cells, IRF-2 colocalized with nucleolin in the peri-nucleolar region. Nucleolin has been reported to colocalize with p53 in a stress-dependent manner; it mobilizes between nucleoli, nuclei and the cytosol depending on the level of stress (Klibanov *et al*., 2001; Daniely *et al*., 2002). This mobilization depends on the cell condition, such as during various stage of growth or differentiation. In our confocal experiment, PCAF expression did not change the localization of either IRF-2 or nucleolin in HeLa cells. In growing and growth-arrested NIH3T3 cells, similar colocalization of nucleolin and IRF-2 is observed. p300/CBP-associated factor-mediated acetylation induces nucleolin-binding affinity to IRF-2 rather than colocalization of both factors.

Treatment with trichostatin A, a typical histone deacetylase inhibitor, enhanced both expression and acetylation of IRF-2 in IRF-2-stably transfected HeLa cells, but the association of IRF-2 with nucleolin was comparable between trichostatin A-treated and untreated HeLa cells (data not shown). Trichostatin A may affect other acetylatable transcription factors, which compete with IRF-2/nucleolin interaction. Alternatively, interaction of PCAF and p300 with IRF-2 may be required for the association of nucleolin and acetylated IRF-2. In fact, as IRF-2 binds PCAF or p300 *in vitro* and *in vivo* as reported earlier (Masumi *et al*., 2003), acetylated IRF-2 may associate with nucleolin together with PCAF or p300. However, the nucleolin recruitment in anti-flag M2 agarose precipitate from flag-tagged PCAF-transfected cells was difficult to detect. From these results it can be concluded that nucleolin binds to IRF-2 directly, but not to PCAF. Acetylated IRF-2 could be detected at the basal level in

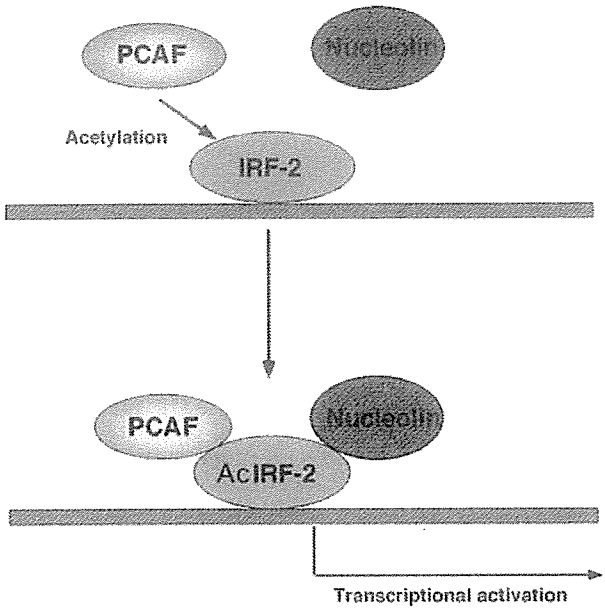

Figure 9 Schematic model of the interferon regulatory factor-2 (IRF-2)-binding complex for its transcriptional regulation. p300/CBP-associated factor (PCAF) acetylates IRF-2, and acetylated IRF-2 associates with endogenous nucleolin together with PCAF. IRF-2/nucleolin/PCAF transactivates the IRF-2-specific promoter.

Figure 8 Nucleolin binds *H4* promoter. (**a**) Laser scanning confocal microscopy was carried out on NIH3T3 cells. Growing or growth-arrested NIH3T3 cells were fixed with paraformaldehyde 24 h after transfection and lysed with 0.2% TritonX-100 for 10 min. Cells were then immunocytostained with a goat anti-interferon regulatory factor-2 (IRF-2) antibody at 4°C overnight and then immunostained with anti-goat second antibody conjugated to Alexa 488 for 2 h (green fluorescence). Following this, washed cells were immunostained with rabbit anti-nucleolin antibody and then anti-rabbit second antibody linked with Alexa 594 (red fluorescence) for 2 h. Washed cells were covered with glycerol and examined by Laser scanning confocal microscopy. Colocalization of proteins results in a merging of red and green fluorescence to produce a yellow image. (**b**) Nucleolin interacts with IRF-2 in growing NIH3T3 cells. Nuclear extracts were prepared from growth-arrested (lanes 1 and 3) and growing NIH3T3 cells (lanes 2 and 4), and incubated with magnetic beads conjugated to *H4* promoter. Bound materials (lanes 1 and 2) and whole nuclear extract (lanes 3 and 4) were analysed by immunoblot assay using anti-nucleolin, anti-IRF-2 and anti-acetyllysine antibodies. (**c**) NIH3T3 cells were transfected with p300/CBP-associated factor (PCAF) and crosslinked with 1% formaldehyde, chromatin was isolated as described under 'Materials and methods' and a chromatin immunoprecipitation assay of the *H4* promoter and glyceraldehyde-3-phosphate dehydrogenase (GAPDH) using anti-IRF-2, anti-nucleolin, anti-PCAF and rabbit immunoglobulin G (IgG) was performed. Polymerase chain reaction (PCR) quantitation was carried out as indicated under 'Materials and methods.'

IRF-2-transfected 293T cells without transfection of PCAF (Figures 1–5). However, we could not detect significant nucleolin recruitment to flag-IRF-2 without transfection of PCAF. p300/CBP-associated factor transfection led to a great extent of nucleolin recruitment instead of slight increase of acetylation of IRF-2, although increasing the extent of PCAF transfection increased nucleolin recruitment and was consistent with IRF-2 acetylation (Figure 5). Acetylated IRF-2 may change its conformation and nucleolin may prefer to bind to acetylated IRF-2. Nucleolin has many acid residues such as glutamic acid and asparagic acid (Lapeyre *et al*., 1987). In contrast, IRF-2 has 18 lysine residues in DNA-binding domain (Masumi *et al*, 2003). We do not at present understand how they associate via their amino acids charge, but expect to be able to determine the binding form for both factors in the future. p300/CBP-associated factor transfection may not only enhance the acetylation but also the binding affinity of IRF-2 with nucleolin. According to the chromatin precipitation analysis, PCAF transfection enhanced nucleolin and IRF-2 binding to *H4* promoter, but PCAF binding to H4 promoter was enhanced only slightly by PCAF transfection. Exogenous PCAF may contribute to the acetylation of IRF-2 rather than an association with *H4* promoter.

As shown in Figure 4b, p300 transfection into cells induced much less amount of nucleolin recruitment to IRF-2 compared to PCAF transfection. Although PCAF appeared to be a slightly better IRF-2 acetylase, transfection of p300 also resulted in substantial acetylation of IRF-2 (Figure 1a). It is not clear why p300 only induced modest recruitment of nucleolin to IRF-2 (Figure 4b), despite fairly high level of IRF-2 acetylation. p300 may acetylate other proteins which compete with IRF-2 for binding to nucleolin. We are currently searching for other acetylated proteins that associate with nucleolin when PCAF or p300 is transfected.

It has been shown that p300 and PCAF interact with and acetylate HIV Tat on distinct lysine residues (Kiernan *et al*., 1999; Ott *et al*., 1999). The acetylation of the activator domain of Tat by PCAF and p300 has different biological functions for Tat, and both events increase the activation of transcription from the LTR (Ott *et al*., 1999, 49). In addition, Chen *et al*. (2002) demonstrated that acetylation of RelA at distinct sites differentially regulates various biological functions of NF-κB. Martinez-Balbas *et al*. (2000) showed that acetylase PCAF, and to a lesser extent CBP and p300, can acetylate E2F1 *in vivo* and increase its DNA-binding ability and that the acetylation status of E2F1 is affected by the histone deacetylase associated with the RB–E2F1 complex. Thus, acetylation of transcription factors leads to changes in their biological activity in terms of DNA-binding affinity, transcriptional activity, interaction with other proteins, and intracellular protein stability (Bannister and Miska, 2000). In the case of IRF-2, we demonstrated that the same sites of IRF-2 were acetylated by PCAF and p300 and that acetylated IRF-2 bound to the promoter more efficiently than non-acetylated IRF-2 *in vivo* as shown earlier (Masumi *et al*., 2003). Acetylated and non-acetylated IRF-2 appear to bind differently to cellular proteins. Acetylated IRF-2 binds to promoters more efficiently, probably by recruiting cellular factors, such as the nucleolin identified in this study.

Barlev *et al*. (2001) showed that acetylated p53 binds more tightly to the transcriptional cofactors transformation/transcription domain-associated protein (TRRAP) and CREB-binding protein than non-acetylated p53, although acetylated and non-acetylated p53 bind to the p21 promoter in the same manner. Levy *et al*. (2004) demonstrated that acetylated β-catenin associates preferentially with Tcf4 (T-cell factor/lymphoid enhancer factor) and that co-activaion of β-catenin/Tcf by p300 is mediated in part by acetylation of β-catenin. In our study, we have confirmed that PCAF-acetylated IRF-2 forms a complex with nucleolin. Histone acetylases such as PCAF and p300 mediate IRF-2-dependent transcriptional activation through nucleolin–IRF-2 interaction. Our findings provide the biological evidence for a transcriptional regulatory mechanism which is effected via protein acetylation.

Materials and methods

Cell culture and transfection

NIH 3T3 cells were grown in Dulbecco's-modified Eagle's medium (DMEM) (Sigma, St. Louis, MI, USA) with 10% calf serum (GIBCO BRL, Rockvile, MD, USA), penicillin (100 U/ml) and streptomycin (100 μg/ml) at 37°C in 5% CO_2 and 95% air. NIH 3T3 cells were transfected with H4 reporter using lipofectamine (Invitrogen, Carlsbad, CA, USA) as described earlier (Masumi *et al*., 2003). For making growth-arrested NIH3T3 cells, DMEM containing 0.5% calf serum was added to growing NIH3T3 cells, and cells were cultured for 48 h. HeLa and 293T cells were grown in DMEM with 10% fetal calf serum (Sigma). 293T cells were then transfected with IRF-2pcDNA3.1, PCAFPCNX and p300pCI plasmids (Masumi *et al*, 1999; Masumi and Ozato, 2001) using Fugene 6 (Roche Biochemicals, Indianapolis, IN, USA). At 24–48 h after transfection, cells were lysed in a buffer B (Tris-HCl, pH 8.0, 0.1 mM ethylenediamine tetraacetic acid (EDTA), 100 mM NaCl, 0.1% NP-40), containing a protease inhibitor mix (Sigma). For some experiments, 20 μCi of ^{14}C-acetate (Amersham, Piscataway, NJ, USA) were added 1 h before preparation of the cell lysate. Cell lysates were used for an anti-flag M2-agarose pull-down assay. K562 cells were cultured in RPMI medium (Sigma) with 10% fetal calf serum. To produce stable transfectants, HeLa and K562 cells were transfected with IRF-2 or IRF-2K75R (Masumi *et al*., 2003) using Fugene 6 (Roche Biochemicals) and cultured for 2 weeks in the presence of 400 μg/ml G418. G418-resistant cells were pooled and lysed for preparation of cell lysate. The nucleolin plasmid was a kind gift from Dr S Murakami (Hirano *et al*., 2003).

Western blotting

Whole cell lysates were prepared in lysis buffer B, with the addition of a protease inhibitor cocktail (Sigma). The insoluble materials and whole cell lysates containing equal amounts of total proteins were suspended in an SDS sample buffer boiled, separated on SDS–10% PAGE, and transferred onto polyvinylidene difluoride membranes (Millipore, Bedford, MA, USA). The membranes were blocked with 5% non-fat dry milk

in a phosphate-buffered saline (PBS)-T buffer (PBS containing 0.5% Tween 20) for 1 h, incubated with anti-IRF-2 (Santa Cruz), anti-p300 (Santa Cruz), anti-acetyl lysine (New England Biology, Beverly, MA, USA) and anti-flag (Sigma) antibodies for 1 h, and washed in PBS-T. The antigen–antibody interaction was visualized by incubation in a chemiluminescent reagent (Perkin Elmer Co. Ltd) and exposure to X-ray film. Immunoblotted membranes were reused for Image analysis using a Fuji BAS 2500 (Fuji Film, Japan) to visualize ^{14}C-incorporated protein.

Affinity DNA-binding assay
The DNA affinity-binding assay was performed as described (Masumi *et al*., 2003). Briefly, nuclear extracts (500 μg of protein) were incubated with magnetic beads conjugated to biotinylated oligonucleotide from the H4 gene. Bound materials were immunoblotted with anti-nucleolin antibody.

Chromatin immunoprecipitation
A total 1×10^7 NIH3T3 cells were crosslinked with 1% formaldehyde for 15 min at room temprature. Cells were washed with PBS and resuspended in 1 ml of lysis buffer (1% SDS, 10 mM EDTA, 50 mM Tris-HCl, pH 8.0) plus a protein inhibitor mixture (Sigma), incubated on ice for 10 min, and sonicated to an average size of 500 bp by an ultrasonic cell disruptor (Ultra 5 homogenizer, TAITEC). Aliquots (100 μl) of sonicated chromatin were diluted in 1 ml of buffer (1%Triton X-100, 2 mM EDTA, 150 mM NaCl, 20 mM Tris-HCl, pH 8) and precleared with 2 μg of sheared salmon sperm DNA and protein G-Sepharose (Invitrogen) for 2 h at 4°C. Immunoprecipitation was performed overnight at 4°C with anti-IRF-2, anti-nucleolin (Santa Cruz) anti-PCAF (UBI) and rabbit immunoglobulin G (IgG) (Sigma). A 50-μl aliquot protein G-Sepharose, and 2 μg of salmon sperm DNA were added to each immunoprecipitation and incubated for 1 h. Precipitates were washed as described earlier and samples were extracted twice with elution buffer (1%SDS, 0.1 M $NaHCO_3$), heated at 65°C to reverse crosslinks, and DNA fragments were purified with phenol/chloroform. A 5-μl aliquot from a total of 30 μl was used in the PCR as descried earlier (Masumi *et al*., 2003).

Purification of interferon regulatory factor-2 precipitates and analysis of mass spectrometry
Cell lysates were prepared from 293T cells transfected with IRF-2 (flag-tag or no-tag) and PCAF (flag-tag or without tag) and incubated with 50–100 μl M2 agarose (Sigma) for 2 h with rotation. After washing with buffer B, bound proteins were eluted from M2 agarose by incubation for 5 min with 30 μl of the flag peptide (0.2 mg/ml) (Sigma) in the same buffer. Eluted protein was separated on SDS–PAGE and stained with Simply blue (Invitrogen). To identify the IRF-2-associated protein, a sliced band from the gel was digested with trypsin and peptides were analysed by LC–MS/MS using LCQ-Deca XP ion trap mass spectrometer (Thermo Electron Corp., Waltham, MA, USA).

M2-agarose pull-down assay
For the M2-agarose pull-down assay, cell lysates from the 293T transfectants were incubated with M2 agarose (Sigma) in buffer B and washed three times. Bound materials were eluted by a 0.2 mg/ml flag peptide (Sigma), resolved on SDS–12.5% PAGE, and detected by Western blotting.

Small interfering RNA experiments
NIH3T3 cells were seeded at density of 3×10^5 cells per ml onto 24-well plate. After 16 h, cells were transfected with 100 mM siRNA oligonucleotides by RNAiFect Transfection Reagent (QIAGEN, Hilden, Germany) and the siRNA-containing medium was removed after 24 h of transfection, and then IRF-2pcDNA3.1, PCAFPCNX with H4 promoter luciferase reporter were transfected into NIH3T3 cells by lipofectamine (Invitrogen). Luciferase activity was analysed 24 h after transfection with plasmids. The sequences of siRNAs used here were as follows: nucleolin, GCUUUAAAUUCCU-GUAAUATT, negative control, non-silencing Alexa Flour 488 Labeled Control siRNA (QIAGEN).

Confocal microscopy
For laser scanning focal microscopy experiments, HeLa cells were cultured in a 35 mm glass bottom dish (Matsunami Glass Ind. Ltd, Japan). At 24 h after transfection, the cells were fixed with paraformaldehyde and lysed with 0.2% TritonX-100 in order to maintain the integrity of the cellular structures. They were then stained with appropriate antibodies as follows: cells transfected with flag-IRF-2 were stained with an anti-flag M2-Cy3 (Sigma). Cells were subsequently stained with anti-nucleolin-linked FITC (Santa Cruz 'sc-8023') for 16 h. NIH3T3 cells were stained with an goat anti-IRF-2 antibody (Santa Cruz) for 16 h and then with an anti-goat second antibody linked to Alexa 488 (Molecular Probes Inc., Eugene, OR, USA) for 2 h. Cells were subsequently stained with rabbit anti-nucleolin antibody (Santa Cruz), and then anti-rabbit IgG-linked Alexa 594 (Molecular Probe Co. Ltd). Stained cells were washed with Tris-buffer saline and mounted on glass slides with a mounting medium (glycerol-PBS). Fluorescent images were collected on a Zeiss Axiovert 100 confocal microscope using a Zeiss $\times 40$ objective.

Acknowledgements

This work was supported by the Japan Society for Promotion of Sciences and the Ministry of Education, Science, Sports and Culture and the Japan Health Sciences International Foundation. We thank Dr Y Nakatani for providing plasmids, Dr K Sakai and Dr M Kasai for technical advices, Dr K Kamemura, Dr A Ito, Dr Y Murakami and Dr I Hamaguchi for useful discussions, and Dr A Fuse and Dr Y Uehera for general support.

References

Bannister AJ, Miska EA. (2000). *Cell Mol life Sci* **57**: 1184–1192.
Barlev N, Liu L, Chehab N, Mansfield K, Harris K, Halazonetis T *et al*. (2001). *Mol Cell* **8**: 1243–1254.
Benkirane M, Chun RF, Xiao H, Ogryzko VV, Howard BH, Nakatani Y *et al*. (1998). *J Biol Chem* **273**: 24898–24905.
Caillaud A, Prakash A, Smith E, Masumi A, Hovanessian A, Levy D *et al*. (2002). *J Biol Chem* **277**: 49417–49421.
Chen L-F, Mu Y, Greene WC. (2002). *EMBO J* **21**: 6539–6548.
Chow W, Fang J, Yee J. (2000). *J Immunol* **164**: 3512–3518.
Daniely Y, Dimitrova DD, Borowiec JA. (2002). *Mol Cell Biol* **22**: 6014–6022.

Deng L, de la Fuente C, Fu P, Wang L, Donnelly R, Wade JD *et al.* (2000). *Virology* **277**: 278–295.
Ginisty H, Sicard H, Roger B, Bouvet P. (1992). *J Cell Sci* **112**: 761–772.
Grinstein E, Wernet P, Snijders PJF, Rosl F, Weinert I, Jia W *et al.* (2002). *J Exp Med* **196**: 1067–1078.
Hamamori Y, Sartorelli V, Ogruzko V, Puri PL, Wu HY, Wang JY *et al.* (1999). *Cell* **96**: 405–413.
Harrod R, Kuo YL, Tang Y, Yao Y, Vassilev A, Nakatani Y *et al.* (2000). *J Biol Chem* **275**: 11852–11857.
Hirano M, Kaneko S, Yamashita T, Luo H, Qin W, Shirota Y *et al.* (2003). *J Biol Chem* **278**: 5109–5115.
Jiang H, Lu H, Schiltz RL, Pise-Masison CA, Ogryzko VV, Nakatani Y *et al.* (1999). *Mol Cell Biol* **19**: 8136–8145.
Kiernan RE, Vanhulle C, Schiltz L, Adam E, Xiao H, Maudoux F *et al.* (1999). *EMBO J* **18**: 6106–6118.
Klibanov S, O'Hagen H, Ljungman M. (2001). *J Cell Sci* **114**: 1867–1873.
Lakin ND, Jackson SP. (1999). *Oncogene* **18**: 7644–7655.
Lang S, Hearing P. (2003). *Oncogene* **22**: 2836–2841.
Lapeyre B, Bourbon H, Amalric F. (1987). *Proc Natl Acad Sci* **84**: 1472–1476.
Lau OD, Coutney AD, Vassilev A, Marzilli LA, Cotter RJ, Nakatani Y *et al.* (2000a). *J Biol Chem* **275**: 21953–21959.
Lau OD, Kundu TK, Soccio RE, Ait-Si-Ali S, Khalil EM, Vassilev A *et al.* (2000b). *Mol Cell* **3**: 589–595.
Levy L, Wei Y, Labalette C, Wu Y, Renard CA, Buendia MA *et al.* (2004). *Mol Cell Biol* **24**: 3404–3414.
Li J, O'Malley BW, Wong J. (2000). *Mol Cell Biol* **20**: 2031–2042.
Luo W, Skalnik DG. (1996). *J Biol Chem* **271**: 23445–23451.
Martinez-Balbas MA, Baner UM, Nielsen SJ, Brehm A, Kouzarides T. (2000). *EMBO J* **19**: 662–671.
Masumi A, Ozato K. (2001). *J Biol Chem* **276**: 20973–20980.
Masumi A, Wang I-M, Lefebvre B, Yang X-J, Nakatani Y, Ozato K. (1999). *Mol Cell Biol* **19**: 1810–1820.
Masumi A, Yamakawa Y, Fukazawa H, Ozato K, Komuro K. (2003). *J Biol Chem* **278**: 25401–25407.
Ott M, Schnolzer M, Gamica J, Fischle W, Emiliani S, Rackwiz HR *et al.* (1999). *Curr Biol* **9**: 1489–1492.
Patel J, Du Y, Ard P, Phillips C, Carella B, Chen C *et al.* (2004). *Mol Cell Biol* **24**: 10826–10834.
Polwsskaya A, Naguibneva I, Duquet A, Bengal E, Robin P, Harel-Bellan A. (2001). *Mol Cell Biol* **21**: 5312–5320.
Santos-Rosa H, Valls1 E, Kouzarides T, Martinez-Balbas M. (2003). *Nucl Acids Res* **31**: 4285–4292.
Schaffer BC, Paulson E, Strominger JL, Speck SH. (1997). *Mol Cell Biol* **17**: 873–886.
Schiltz RL, Mizzen CA, Vassilev A, Cook RG, Allis CD, Nakatani Y. (1999). *J Biol Chem* **274**: 1189–1192.
Spilianakis C, Papamatheakis J, Kretsovail A. (2000). *Mol Cell Biol* **20**: 8489–8498.
Srivastava M, Pollard HB. (1999). *FASEB J* **13**: 1911–1922.
Stellacci E, Testa U, Retrucci E, Benedetti E, Orsatti R, Feccia T *et al.* (2004). *Biochem J* **377**: 367–378.
Sterner DE, Berger SL. (2000). *Mol Cell Biol* **64**: 435–459.
Suhara W, Yoneyama M, Kitabayashi I, Fujita T. (2002). *J Biol Chem* **277**: 22304–22313.
Taniguchi T, Ogasawara K, Takaoka A, Tanaka N. (2001). *Annu Rev Immunol* **19**: 623–655.
Trievel RC, Li FY, Mamorstein R. (2000). *Anal Biochem* **287**: 319–328.
Vassilev A, Yamauchi J, Kotani T, Prives C, Avantaggiati ML, Qin J *et al.* (1998). *Mol Cell* **2**: 869–875.
Vaughan PS, van der Meijden CM, Aziz F, Harada H, Taniguchi T, van WA *et al.* (1998). *J Biol Chem* **273**: 194–199.
Vo N, Goodman RH. (2001). *J Biol Chem* **276**: 13505–13508.
Wang I-M, Blanco JCG, Tsai SY, Tsai M-J, Ozato K. (1996). *Mol Cell Biol* **16**: 6313–6324.
Wolf D, Rodova M, Miska EA, Calvet JP, Kouzarides T. (2002). *J Biol Chem* **28**: 25562–25567.
Xie R, van Wijnen AJ, van der Meijden C, Luong MX, Stein JL, Stein GS. (2001). *J BIol Chem* **276**: 18624–18632.
Yamamoto H, Lamphier M, Fujita T, Taniguchi T, Harada H. (1994). *Oncogene* **9**: 1423–1428.
Yamauchi T, Yamauchi J, Kuwata T, Tamura T, Yamashita T, Bae N *et al.* (2000). *Proc Natl Acad Sci USA* **97**: 11303–11306.
Yanagida M, Shimamoto A, Nishikawa K, Furuichi Y, Takahashi N. (2001). *Proteomics* **1**: 1390–1404.
Ying G-G, Proost P, van Damme J, Bruschi M, Introna M, Golay J. (2000). *J Biol Chem* **275**: 4152–4158.
Yoneyama M, Suhara W, Fukuhara Y, Fukuda M, Nishida E, Fujita T. (1998). *EMBO J* **17**: 1087–1095.

Available online at www.sciencedirect.com
SCIENCE DIRECT
ELSEVIER
Journal of Virological Methods 136 (2006) 254–256
Journal of Virological Methods
www.elsevier.com/locate/jviromet

Short communication

Evaluation of 10 commercial diagnostic kits for in vitro expressed hepatitis B virus (HBV) surface antigens encoded by HBV of genotypes A to H

Toshiaki Mizuochi *, Yoshiaki Okada, Kiyoko Umemori, Saeko Mizusawa, Kazunari Yamaguchi

Department of Safety Research on Blood and Biological Products, National Institute of Infectious Diseases, 4-7-1 Gakuen Musashi-Murayama-shi, Tokyo 208-0011, Japan

Received 26 January 2006; received in revised form 15 March 2006; accepted 21 March 2006
Available online 16 May 2006

Abstract

Genetic variability of the hepatitis B virus (HBV) constitutes one of the major challenges for diagnosis of HBV infection. It is plausible that amino acid substitutions in the "a" determinant of the HBV surface antigen (HBsAg) that affect antigenic sites, whether originating from genetic diversity or from mutations in the HBV strain itself, will affect the sensitivity of some diagnostic kits. In fact, recent studies have indicated that some diagnostic kits had false negative results with particular HBsAg mutants. There have been, however, few substantial studies evaluating sensitivities of diagnostic kits to the HBsAg encoded by different HBV genotypes. Our recent study found that 10 diagnostic kits available in Japan were able to detect HBsAg irrespective of whether it originated from HBV genotypes A, B or C, with the latter two genotypes being the dominant species in East Asia. In this study, we extended our previous efforts by assessing the ability of diagnostic kits to detect recombinant HBsAg derived from HBV genotypes A to H. Our results demonstrated that 9 out of 10 diagnostic kits evaluated were able to detect as low as 0.2 International Units (IU)/ml HBsAg, irrespective of HBV genotype. The genotypic differences in the HBV family thus appear to have little impact on the sensitivity of currently available HBsAg diagnostic kits.

Keywords: HBsAg: Diagnostic kits: HBV genotype

Based on an intergroup divergence of 8% or more in the complete nucleotide sequence of approximately 3200 nucleotides, HBV has been classified into eight genotypes, designated as A to H (Okamoto et al., 1988; Norder et al., 1994; Stuyver et al., 2000; Arauz-Ruiz et al., 2002). The prevalence of specific genotypes varies geographically: genotypes A and D are widely distributed throughout the Old World, while genotypes B and C are dominant in East Asia. Furthermore, the distribution of HBV genotypes may vary over time and with population migration. It is therefore critical for diagnostic kits to be able to detect HBsAg encoded by various HBV genotypes with comparable sensitivity. Moreover, given the accumulating body of evidence that certain HBV genotypes correlate with disease features and treatment outcomes, including the severity of liver disease (Mayerat et al., 1999; Kao et al., 2000a; Orito and Mizokami, 2003), HBe antigen seroconversion (Chu et al., 2002; Ishikawa et al., 2002), and susceptibility to anti-viral drugs (Kao et al., 2000b; Wai et al., 2002; Kao et al., 2002; Zollner et al., 2004), from a treatment perspective the specificity and sensitivity of assays for sub-typing HBV genotypes is also critical. In our previous report (Mizuochi et al., 2005), we evaluated the sensitivity of 10 diagnostic kits to serum/plasma samples containing HBsAg as well as recombinant HBsAg encoded by HBV of genotypes A, B, and C. None of the diagnostic kits examined failed to detect HBsAg of genotypes A, B, and C at the concentration of 0.2 IU/ml. Furthermore, there was no difference between naturally derived antigens, i.e. serum/plasma samples, and recombinant antigens in the outcome of assays. In the present study, we sought to extend our previous study by evaluating the same diagnostic kits for their sensitivity to HBsAg encoded by HBV of all the genotypes reported to date, i.e. A to H.

Plasma specimens of HBV Genotypes A and D were obtained from International Reagents Corporation (Kobe, Japan).

Abbreviations: HBV, Hepatitis B virus; HBsAg, Hepatitis B virus surface antigen; IU, International unit

* Corresponding author. Tel.: +81 42 561 0771; fax: +81 42 562 7892.
E-mail address: miz@nih.go.jp (T. Mizuochi).

0166-0934/$ – see front matter © 2006 Elsevier B.V. All rights reserved.
doi:10.1016/j.jviromet.2006.03.022

Table 1
HBsAg diagnostic kits used in this study

No.	Method	Antibody (capture/detection)
1	CLIA	Monoclonal/polyclonal
2	EIA	Monoclonal/polyclonal
3	CLIA	Monoclonal/polyclonal
4	EIA	Monoclonal/polyclonal
5	EIA	Monoclonal/monoclonal(×2)[a]
6	CLEIA	Polyclonal/monoclonal(×2)[a]
7	CLEIA	Monoclonal/monoclonal(×2)[a]
8	EIA	Polyclonal/monoclonal
9	CLIA	Monoclonal/monoclonal
10	CLIA	Monoclonal/monoclonal

CLIA: Chemiluminescent immunoassay: EIA: enzyme immunoassay: CLEIA: chemiluminescent enzyme immunoassay.
[a] (×2): Two different monoclonal antibodies.

Table 2
HBsAg diagnostic kits used in this study listed in alphabetical order of manufacturers

Product name	Manufacturer
AxSYM HBsAg	Abbott Japan Co. Ltd.
IMx HBsAg	Abbott Japan Co. Ltd.
ARCHITECT HBsAg	Abbott Japan Co. Ltd.
PRISM HBsAg	Abbott Japan Co. Ltd.
ADVIA Centaur HBsAg Assay	Bayer Medical Ltd.
VIDAS HBsAg Ultra	bioMerieux Japan Ltd.
Monolisa HBsAg	Bio-Rad Fujirebio
Lumipulse II HBsAg	FUJIREBIO INC.
Vitros Immunodiagnostics	Ortho-Clinical
Products HBsAg Reagent Pack	Diagnostics K.K.
Elecsys HBsAg	Roche Diagnostics K.K.

Note: The order of kits in this table is not corresponding to that of Table 1.

Genotypes B and C were kindly supplied by Taiwan FDA and Japanese Red Cross, respectively. Genotypes E, F, G, and H were purchased from Teragenix Co. (Ft. Lauderdale, FL, USA). All the HBV full genomes except for genotype H were cloned into plasmids by the method described by Günther et al. (1995). All the plasmids containing HBV full genomes were able to produce HBsAg in culture supernatant by transfection into HuH-7 cells (Nakabayashi et al., 1982) with lipofectin reagent (Invitrogen Co., San Diego, CA, USA). The amount of HBsAg produced by each genotype of HBV is highly variable, depending on the promoter activity of each clone (data not shown). To minimize this variation among the genotypes, S genes were amplified by PCR from plasmids containing HBV full genomes and then cloned into the pEF6/V5-His (Invitrogen Co., San Diego, CA, USA) which has the elongation factor-1α promoter to express the inserted S genes. The S gene of genotype H was amplified with DNA extracted from the plasma sample by PCR and cloned into the same plasmid. The genotypes of all the cloned S genes were determined by sequencing. Three micrograms plasmid of each genotype were transfected into 2×10^5 HuH-7 cells/well in a six-well culture plate (Asahi Technoglass Co., Chiba, Japan) with 10 μg lipofectin reagent (Invitrogen Co., San Diego, CA, USA), and the cells were cultured at 37 °C in 5% CO_2. Culture supernatants were harvested after 3 days and stored at −20 °C until use.

The concentration of each recombinant HBsAg sample was tentatively determined by utilizing ARCHITECT HBsAg QT (Abbott Japan Co. Ltd., Chiba, Japan), which is the only quantitative assay kit approved in Japan, and expressed in IU/ml. The concentration of each sample was adjusted to 10 IU/ml with a multi-marker negative matrix (Accurun 810; BBI Co. Ltd., Boston, MA, USA). The samples were subsequently diluted to make two different concentrations (0.2 and 1.0 IU/ml). These test samples of various HBV genotypes were analyzed with 10 diagnostic kits as listed in Tables 1 and 2. Tests were performed according to the manufacturer's instruction and results were expressed as C.O.I. (cut-off index) as shown in Fig. 1A and B. All of the HBsAg samples, irrespective of their HBV genotype, tested positively in all assay kits at the concentration of 1.0 IU/ml (Fig. 1A). When the HBsAg samples at the lower concentration (0.2 IU/ml) were tested, 9 out of 10 kits gave positive results. Only one kit (No. 8) gave negative results for the HBsAg of genotypes E and F (Fig. 1B). This sensitivity (0.2–1.0 IU/ml) approaches the satisfactory criterion according to the "Guidance for Industry" issued by the FDA or the "CTS" (Common Technical Specification) defined by the EU. Only one kit failed to give positive results for the low concentration of HBsAg (0.2 IU/ml) encoded by the HBV of genotypes E and F (Fig. 1B). The results shown in this study thus confirmed the sensitivity of currently available diagnostic kits to HBsAg encoded by HBV of genotypes A to H.

Since HBsAg genotypes F and H are genetically distant from the other six genotypes (Norder et al., 2004), concerns have been raised as to the ability of the detection of these genotypes by currently available diagnostic kits. The data in this study

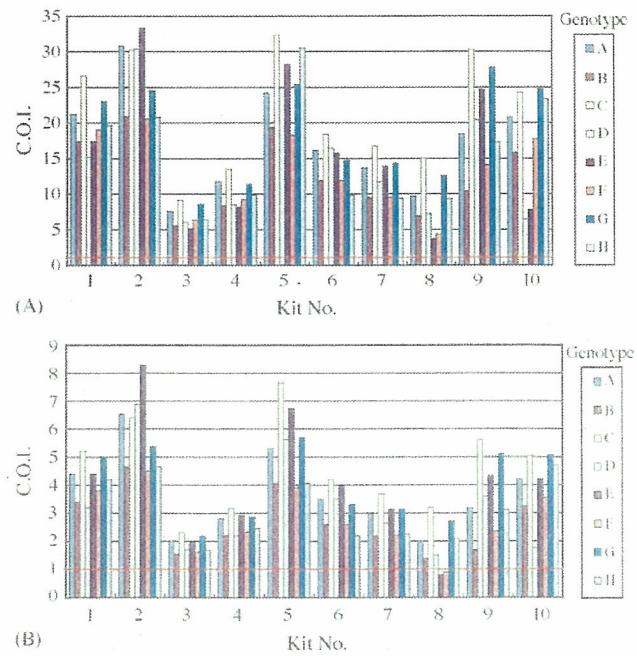

Fig. 1. Detection of recombinant HBsAg (A: 1.0 IU/ml, B: 0.2 IU/ml) derived from HBV of genotypes A to H were assayed by utilizing 10 diagnostic kits listed in Tables 1 and 2. Results were expressed as C.O.I. (cut-off index). The inserted horizontal lines indicate "C.O.I. = 1.0".

show that 9 out of 10 kits tested are capable of detecting as low as 0.2 IU/ml HBsAg including HBV genotypes F and H, alleviating this concern.

Acknowledgments

We are grateful to the manufacturers who kindly supplied us with the HBsAg diagnostic kits and helped us in performing the assays.

References

Arauz-Ruiz, P., Norder, H., Robertson, B.H., Magnius, L.O., 2002. Genotype H: a new Amerindian genotype of hepatitis B virus revealed in Central America. J. Gen. Virol. 83, 2059–2073.

Chu, C.J., Hussain, M., Lok, A.S., 2002. Hepatitis B virus genotype B is associated with earlier HBeAg seroconversion compared with hepatitis B virus genotype C. Gastroenterology 122, 1756–1762.

Günther, S., Li, B.-C., Miska, S., Kruger, D.H., Meisel, H., Will, H., 1995. A novel method for efficient amplification of whole hepatitis B virus genomes permits rapid functional analysis and reveals deletion mutants in immunosuppressed patients. J. Virol. 69, 5437–5444.

Ishikawa, K., Koyama, T., Masuda, T., 2002. Prevalence of HBV genotypes in asymptomatic carrier residents and their clinical characteristics during long-term follow-up: the relevance to changes in the HBeAg/anti-HBe system. Hepatol. Res. 24, 1–7.

Kao, J.H., Chen, P.J., Lai, M.Y., Chen, D.S., 2000a. Hepatitis B genotypes correlate with clinical outcomes in patients with chronic hepatitis B. Gastroenterology 118, 554–559.

Kao, J.H., Wu, N.H., Chen, P.J., Lai, M.Y., Chen, D.S., 2000b. Hepatitis B genotypes and the response to interferon therapy. J. Hepatol. 33, 998–1002.

Kao, J.H., Liu, C.J., Chen, D.S., 2002. Hepatitis B viral genotypes and lamivudine resistance. J. Hepatol. 36, 303–304.

Mayerat, C., Mantgegani, A., Frei, P.C., 1999. Does hepatitis B virus (HBV) genotype influence the clinical outcome of HBV infection? J. Viral Hepat. 6, 299–304.

Mizuochi, T., Okada, Y., Umemori, K., Mizusawa, S., Sato, S., Yamaguchi, K., 2005. Reactivity of genotypically distinct hepatitis B virus surface antigens in 10 commercial diagnostic kits available in Japan. Jpn. J. Inf. Dis. 58, 83–87.

Nakabayashi, H., Taketa, K., Miyano, K., Yamane, T., Sato, J., 1982. Growth of human hepatoma cells lines with differentiated functions in chemically defined medium. Cancer Res. 42, 3858–3863.

Norder, H., Courouce, A.M., Magnius, L.O., 1994. Complete genomes, phylogenetic relatedness, and structural proteins of six strains of the hepatitis B virus, four of which represent two new genotypes. Virology 198, 489–503.

Norder, H., Courouce, A.-M., Coursaget, P., Echevarria, J.M., Lee, S.-D., Mushahwar, I.K., Robertson, B.H., Locarnini, S., Magnius, L.O., 2004. Genetic diversity of hepatitis B virus strains derived worldwide: genotypes, subgenotypes, and HBsAg subtypes. Intervirology 47, 289–309.

Okamoto, H., Tsuda, F., Sakugawa, H., Sastrosoewignjo, R.I., Imai, M., Miyakawa, Y., Mayumi, M., 1988. Typing hepatitis B virus by homology in nucleotide sequence: comparison of surface antigen subtypes. J. Gen. Virol. 69, 2575–2583.

Orito, E., Mizokami, M., 2003. Hepatitis B virus genotypes and hepatocellular carcinoma in Japan. Intervirology 46, 408–412.

Stuyver, L., De Gendt, S., Van Geyt, C., Zoulim, F., Fried, M., Schinazi, R.F., Rossau, R., 2000. A new genotype of hepatitis B virus: complete genome and phylogenetic relatedness. J. Gen. Virol. 81, 67–74.

Wai, C.T., Chu, C.J., Hussain, M., Lok, A.S., 2002. HBV genotype B is associated with better response to interferon therapy in HBeAg(+) chronic hepatitis than genotype C. Hepatology 36, 1425–1430.

Zollner, B., Petersen, J., Puchhammer-Stockl, E., Kletzmayr, J., Sterneck, M., Fischer, L., Schroeter, R., Feucht, H.H., 2004. Viral features of lamivudine resistant hepatitis B genotypes A and D. Hepatology 39, 42–50.

Loss of Tie2 receptor compromises embryonic stem cell–derived endothelial but not hematopoietic cell survival

Isao Hamaguchi, Tohru Morisada, Masaki Azuma, Kyoko Murakami, Madoka Kuramitsu, Takuo Mizukami, Kazuyuki Ohbo, Kazunari Yamaguchi, Yuichi Oike, Daniel J. Dumont, and Toshio Suda

Tie2 is a receptor-type tyrosine kinase expressed on hematopoietic stem cells and endothelial cells. We used cultured embryonic stem (ES) cells to determine the function of Tie2 during early vascular development and hematopoiesis. Upon differentiation, the ES cell–derived Tie2$^+$Flk1$^+$ fraction was enriched for hematopoietic and endothelial progenitor cells. To investigate lymphatic differentiation, we used a monoclonal antibody against LYVE-1 and found that LYVE-1$^+$ cells derived from Tie2$^+$Flk1$^+$ cells possessed various characteristics of lymphatic endothelial cells. To determine whether Tie2 played a role in this process, we analyzed differentiation of *Tie2*$^{-/-}$ ES cells. Although the initial numbers of LYVE-1$^+$ and PECAM-1$^+$ cells derived from *Tie2*$^{-/-}$ cells did not vary significantly, the number of both decreased dramatically upon extended culturing. Such decreases were rescued by treatment with a caspase inhibitor, suggesting that reductions were due to apoptosis as a consequence of a lack of Tie2 signaling. Interestingly, *Tie2*$^{-/-}$ ES cells did not show measurable defects in development of the hematopoietic system, suggesting that Tie2 is not essential for hematopoietic cell development. (Blood. 2006;107:1207-1213)

Introduction

A close cell lineage relationship between hematopoietic and endothelial cells has long been recognized.[1,2] During embryogenesis, both cell types emerge in the yolk sac, and primitive erythrocytes differentiate juxtaposed to endothelial precursors by embryonic day 7.5 (E7.5).[3] In the mouse embryo, Tie2$^+$ cells in the aorta-gonad-mesonephros (AGM) region generate both blood and endothelial cells.[4] From studies of embryonic stem (ES) cell differentiation, vascular endothelial growth factor (VEGF)–responsive bipotent precursors of hematopoietic and endothelial cells, known as hemangioblasts, have been identified.[5] Hemangioblast-derived endothelial cells form vascular vessels through vasculogenesis and angiogenesis. Lymphatic development starts when a subset of vascular endothelial cells of the cardinal vein commit to a lymphatic lineage and sprout to form the primary lymph sacs at around E9 or 10.[6,7] Mouse molecular genetic experiments indicate that Prox-1 (a homeobox transcription factor) and the VEGF receptor 3 (VEGFR-3) are crucial for the commitment of endothelial cells to a lymphatic lineage.[8-10] Since lymphatic vessel–specific molecules are being identified, the molecular mechanisms underlying development of lymphatic cells as well as vascular and hematopoietic cells can now be analyzed.

Many studies report that expression of Flk1 is crucial for early establishment of endothelial and hematopoietic lineages and perhaps for their common progenitor.[5,11,12] Flk1 encodes a receptor tyrosine kinase for the vascular endothelial growth factor family of ligands.[13] Single Flk1$^+$ cells from embryoid bodies can give rise to blast colonies (blast lymphocyte colony-forming cells [BL-CFCs]), which produce both hematopoietic and endothelial cells in vitro.[5] Loss of Flk1 in mice results in selective defects in generating both blood and blood-vessel endothelial cells (BECs).[11] In addition to Flk1, Flt1 and Tie2 tyrosine kinases are also expressed in immature hematopoietic cells and BECs.[14-17]

The expression pattern of Tie2 suggests a function in both vascular endothelial and hematopoietic cells. Recently we determined the function of Ang1/Tie2 signaling, which maintains long-term repopulating hematopoietic stem cells in the bone marrow niche, suggesting that Tie2 signaling is crucial for adult bone marrow hematopoiesis.[18] In the mouse vitelline artery at E9.5, Tie2$^+$ hematopoietic cells aggregate and adhere to endothelial cells.[19] In vitro culture of Tie2$^+$ cells isolated from the AGM region generates both blood and endothelial cells.[4] In fetal liver, the Tie2$^+$ fraction contains an enriched fraction of long-term repopulating cells.[20] Based on these findings, Tie2 signaling was thought to regulate embryonic development and differentiation of hematopoietic cells. However, more recently, Puri and Berstein have demonstrated that Tie2 is dispensable for embryonic hematopoiesis using ES cell mouse chimeras.[21] This finding suggests that Tie2 function in developmental hematopoiesis differs from its role in bone marrow hematopoiesis.

From the Department of Cell Differentiation, The Sakaguchi Laboratory, School of Medicine, Keio University, Tokyo, Japan; Department of Safety Research on Blood and Biological Products, National Institute of Infectious Diseases, Tokyo, Japan; Department of Medical Biophysics, University of Toronto, ON, Canada; and the Division of Molecular and Cellular Biology Research, Sunnybrook and Women's Research Institute, Toronto, ON, Canada.

Submitted May 5, 2005; accepted September 27, 2005. Prepublished online as *Blood* First Edition Paper, October 11, 2005; DOI 10.1182/blood-2005-05-1823.

Supported in part by Grants-in-Aid from Ministry of Education, Science, Technology, Sports, and Culture, Japan; and by a research grant from the Human Frontiers Science Program Organization.

Reprints: Isao Hamaguchi, Department of Safety Research on Blood and Biological Products, National Institute of Infectious Diseases, 4-7-1 Gakuen, Musashimurayama, Tokyo 208-0011, Japan; e-mail: 130hama@nih.go.jp; or Toshio Suda, The Sakaguchi Laboratory of Developmental Biology School of Medicine, Keio University, Shinanomachi 35, Shinjuku, Tokyo 160-8582, Japan; e-mail: sudato@sc.itc.keio.ac.jp.

The publication costs of this article were defrayed in part by page charge payment. Therefore, and solely to indicate this fact, this article is hereby marked "advertisement" in accordance with 18 U.S.C. section 1734.

By contrast, Tie2 function in BECs has been intensively analyzed at both developmental and adult stages. In vivo and in vitro experiments show that Tie2 signaling potently induces sprouting, chemotaxis, and network formation.[22,23] Furthermore, the Tie2 ligand Ang1 is a potent survival factor for BECs under serum deprivation.[24] A role for Tie2 signaling in blood vessel endothelial survival in vivo has also been illustrated using conditional rescue of *Tie2*$^{-/-}$ embryos,[25] further supporting a role of this signaling system in endothelial cell survival.

Recently it has been demonstrated in mice that Tie2 is expressed and functions in lymphatic vessels embryonically[26] and in adults.[27] Tie2-deficient mice exhibit severe defects in vascular and heart development and die by E9.5,[28,29] making analysis of the lymphatic system difficult. Therefore, here we analyzed the function of Tie2 in lymphatic endothelial cells (LECs) and hematopoietic cells as well as in developing BECs using differentiation of cultured ES cells. We identify ES cell–derived LECs as well as BECs and hematopoietic cells, and demonstrate that Tie2 signaling is essential for development of BECs and LECs, but not for hematopoietic cells.

Materials and methods

Cell preparation and culture conditions

TT2,[30] E14,[31] and R1[32] ES cells were maintained on mouse embryonic fibroblast (MEF) feeder cell layers in knockout Dulbecco-modified Eagle medium (Gibco BRL, Carlsbad, CA) containing 15% fetal bovine serum (Intergen, Purchase, NY), 100 U/mL leukemia inhibitory factor (LIF; Chemicon International, Temecula, CA), 0.1 mM nonessential amino acids (Gibco BRL), 1 mM sodium pyruvate (Gibco BRL), 2 mM L-glutamine (Gibco BRL), and 100 μM 2-mercaptoethanol (Sigma-Aldrich, St Louis, MO). After removal of LIF, ES cells were cultured on collagen type IV plates (Becton Dickinson, San Jose, CA) at 1×10^4 cells/mL for 2 days. Cells were then disaggregated by trypsin and seeded on OP9 cells at 1×10^5 cells/mL. After 5 days of culture, OP9 cells were removed from ES cells through a Sephadex G10 column (Amersham Bioscience, Uppsala, Sweden), and the ES cells were fractionated by Flk1 and Tie2 expression using FACSvantage (Becton Dickinson). Sorted cells were seeded on OP9 cells at 1000 to 15 000 cells/mL and cultured in the presence of VEGF-C (100 ng/mL; R&D Systems, Minneapolis, MN), VEGF-D (100 ng/mL; R&D Systems), or the caspase inhibitor Z-VAD-fmk (10-100 nM; Calbiochem, La Jolla, CA). When indicated, sorted cells were cultured with recombinant soluble Tie2-Fc fusion protein (30 μg/mL)[19] or recombinant soluble CD4-Fc fusion protein (30 μg/mL).[19]

Immunocytochemistry

Immunocytochemistry was performed essentially as described.[33] Differentiated ES cells cultured on OP9 cells were fixed with 4% paraformaldehyde at 4°C and stained with a rat monoclonal anti-mouse platelet–endothelial cell adhesion molecule 1 (PECAM-1) monoclona antibody (mAb) (MEC13.3; Becton Dickinson) or a rat monoclonal anti-mouse LYVE-1 antibody (ALY7[26]) by the indirect immunoperoxidase method using horseradish peroxidase–conjugated anti-rat IgG. Peroxidase activity was visualized using 3,3′-diaminobenzidine (Dojindo, Kumamoto, Japan). To determine whether Prox-1 was expressed in LYVE-1$^+$ cells, we stained cells with biotinylated ALY7 and anti–Prox-1 antibody (Covance, Berkeley, CA). LYVE-1 and Prox-1 expression was detected by reacting with Alexa 488–conjugated Streptavidin (Molecular Probes, Eugene, OR) and Alexa 546–conjugated goat anti-rabbit antibody (Molecular Probes), respectively. For nuclear staining, cells were treated with TOTO3 (Molecular Probes). Stained cells were visualized by fluorescence microscopy. Stained and unstained cells were visualized by fluorescent microscopy (IX71) with either UplanApo 4×/0.13 NA, 10×/0.40 NA, or 20×/0.70 NA objectives (Olympus, Tokyo, Japan). Images were further processed with Adobe Photoshop (Adobe Systems, San Jose, CA). For DiI labeling, 10 μg/mL DiI-Ac-LDL (Molecular Probes) was added to differentiated ES cells on OP9 cells and adherent cells were incubated for 4 hours at 37°C. After removing the media containing DiI-Ac-LDL, cells were washed and stained with anti–PECAM-1 (FITC-conjugated; Becton Dickinson) or anti–LYVE-1 (biotin-conjugated) plus FITC-conjugated Streptavidin (Becton Dickinson). Uptake of DiI-Ac-LDL by blood vessel endothelial cells (PECAM-1$^+$ cells) and lymphatic endothelial cells (LYVE-1$^+$ cells) was visualized using a standard rhodamine excitation emission filter (Olympus, Tokyo, Japan).

RT-PCR analysis

Total RNA was extracted from cells using RNeasy Kit (Qiagen, Hilder, Germany). Isolated RNA was reverse-transcribed using an reverse transcriptase (RT) for polymerase chain reaction (PCR) Kit (Clontech, Palo Alto, CA). cDNAs were amplified using Taq polymerase (TaKaRa, Kyoto, Japan). Sequences of gene-specific primers for RT-PCR were as follows: *GATA2*, 5′-(acacaccacccgatacccacctat), 3′-(cctacgccatggcagtcaccatgct); *SCL*, 5′-(cgcggatccacggagcggccgccgagcgcg), 3′-(cggaattccgcgccgcactacttggtgtg); c-myb, 5′-(gacagaagaggaggacagaatca), 3′-(tctcagggtcttcgtcgtatag); *AML1*, 5′-(ccagcaagctgaggagcggcg), 3′-(cggatttgtaaagacggtga); *Tie2*, 5′-(ttagttctctgtggagtcag), 3′-(aggccctgagttcttcactc); *Flk1*, 5′-(agaacaccaaaagagaggaacg), 3′-(gcacacaggcagaaaccagtag); *VEGFR3*, 5′-(gctaccactgctactacaag), 3′-(gataatcccagtcgaaggtg); *Prox1*, 5′-(aagtggttcagcaatttccg), 3′-(tgaccttgtaaatggccttc); *LYVE1*, 5′-(ttcctcgcctctatttggac), 3′-(tctgttgtctgcgtttcatcc); *Pdpn*, 5′-(gtgccagtgttgttctgggt), 3′-(tctgttgtctgcgtttcatcc); *Evil*, 5′-(aatatgagtcatgccaaccc), 3′-(cttggtgtactgacatcatc); and *GAPDH*, 5′-(aatcccatcaccatcttcca), 3′-(ccaggggtcttactccttg).

PCR products were separated on a 1.2% agarose gel and gels were stained with ethidium bromide.

Quantitative RT-PCR analysis

Total RNA was isolated from 10^4 cells and cDNA was reverse-transcribed using Superscript III (Invitrogen, Carlsbad, CA) according to the manufacturer's instructions. The expression levels of Ang1, Ang2, and Ang3 were analyzed by quantitative (Q) RT-PCR using a LightCycler instrument (Roche Diagnostics, Mannheim, Germany) with LightCycler software version 3.5. cDNA was amplified for Q-PCR using SYBR Green I (Sigma-Aldrich) to detect PCR product. cDNA (2 μL) was used in a 20-μL final volume reaction containing 10 μL SYBR Premix Ex Taq (TaKaRa), 0.4 μM *Ang1* forward (5′-GCCTTTGCACTAAAGAAGGTGTTTT-3′), and 0.4 μM *Ang1* reverse (5′-ATACATCCGCACAGTCTCGAAATG-3′). The LightCycler was programmed to run an initial denaturation step at 95°C for 10 seconds followed by 45 cycles of denaturation (95°C for 5 seconds) and extension (60°C for 20 seconds), monitoring the synthesis of product at the end of the extension step of each cycle. The same conditions were used with primers *Ang2* forward (5′-AGGAGATCAAGGCCTACTGTGACA-3′) and *Ang2* reverse (5′-GCTCCCGAA GCCCTCTTTG-3′), and *Ang3* forward (5′-GTTCCAGGACTGTGCAGAGATCA-3′) and *Ang3* reverse (5′-TCTCCATGTCACAGAACACCTTGAG-3′). The Ang1, Ang2, and Ang3 values were normalized against mouse β-actin (forward 5′-CAGCCTTCCTTCTTGGGTATGG-3′; reverse 5′-CTGTGTTGGCATAGAGGTC TTTACG-3′).

Flow cytometric analysis and cell sorting

The following mAbs used for flow cytometry were purchased from Becton Dickinson: anti-CD34 (RAM34), anti–c-Kit (ACK45), anti–Sca-1 (E13-161.7), anti–CD45 (30-F11), anti–Flk1 (Avas12α1), anti–PECAM-1 (MEC13.3), anti–Mac-1 (M1/70), anti–Gr-1 (RB6-8C5), and anti–TER-119. Also used were anti-Tie2 mAb (TEK4)[34] and anti–LYVE-1 mAb (ALY7).[26] Fluorescence-activated cell sorting (FACS) analysis was performed on a FACSvantage (Becton Dickinson).

Progenitor assay by methylcellulose culture

Tie2$^+$Flk1$^+$ or Flk1$^+$ cells derived from ES cells were embedded in 1 mL alpha medium containing 1.3% methylcellulose (1500 cp; Sigma-Aldrich), 30% fetal calf serum (FCS), 1% deionized bovine serum albumin (BSA;

Sigma-Aldrich), 0.1 mM 2-mercapto-ethanol (Sigma-Aldrich), 10 ng/mL stem cell factor (SCF; PeproTech EC, London, United Kingdom), 10 ng/mL recombinant mouse interleukin-3 (IL-3; PeproTech EC), 10 ng/mL recombinant human IL-6 (PeproTech EC), and 2 U/mL recombinant human erythropoietin (Epo; Chugai Pharmaceutical, Tokyo, Japan). Cells were cultured in a 35-mm culture dish and incubated at 37°C in a humidified atmosphere with 5% CO_2.

Statistics

Data are expressed as means plus or minus standard deviation (SD). Statistical analysis was conducted using the Student *t* test. Statistical significance was defined as a *P* value less than .05.

Results

In vitro differentiation of ES cells

In order to analyze the function of Tie2 in the development of LECs as well as BECs and hematopoietic cells, we developed a cell culture system for ES cell differentiation. After removal of LIF, E14 ES cells were cultured on collagen type IV plates for 2 days to initiate differentiation to a mesoderm lineage; subsequently, cells were transferred to OP9 stromal cells. Markers of both endothelial and hematopoietic cells, Sca-1, c-kit, and CD34, were expressed in undifferentiated ES cells (Figure 1A). Although 1% of ES cells expressed Flk1 on collagen plates, Tie2 was not expressed in Flk1$^+$ cells (data not shown). Following transfer of cells on collagen plates to OP9 cells, 8% of Flk1$^+$ cells expressed Tie2 on day 3 of culture. Numbers of Tie2$^+$ cells increased until day 5 of culture, when Tie2 expression was maximal; thereafter, both expression levels and numbers of Tie2$^+$ cells gradually decreased. At day 9 of culture, cells cocultured with OP9 cells began expressing CD45, a marker of all hematopoietic cells except mature erythrocytes. Since Tie2$^+$ cells appeared just before CD45$^+$ hematopoietic cells, Tie2$^+$ cells in the Flk1$^+$ cell fraction may represent hematopoietic progenitor cells. We examined other ES strains, such as TT2 and R1 cells, using the same culture conditions, and confirmed that these strains showed a similar mesodermal phenotypes as E14 cells (data not shown).

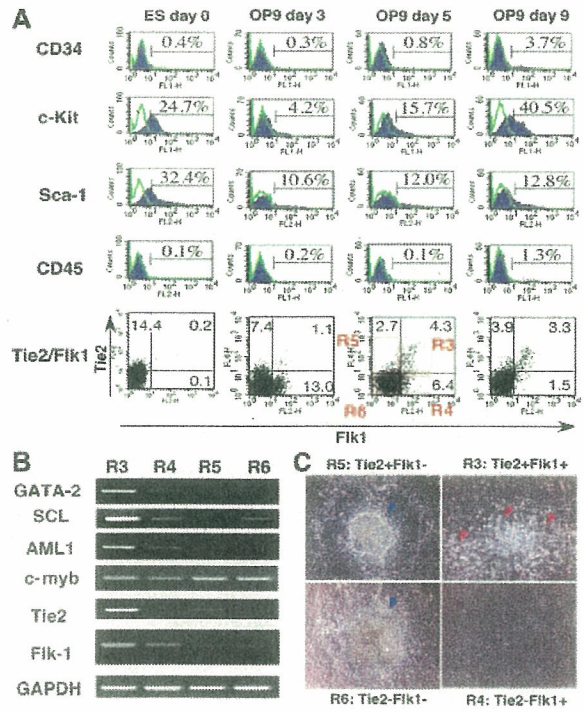

Figure 1. Mesodermal differentiation of ES cells on OP9 stromal cells. (A) E14 ES cells were cultured on collagen type IV plates for 2 days, and then all cells were cultured on OP9 cells for 9 days. The expression of CD34, c-Kit, Sca-1, CD45, Flk1, and Tie2 in ES cell–derived cells was analyzed at the indicated time points by flow cytometry. Stained *Tie*$^{-/-}$ cells are represented by purple shaded histograms. Unstained controls are represented by green lines. The percentages of cells in each quadrant are indicated. (B) Gene expression of fractionated cells shown in A (R3-R6) was analyzed by RT-PCR. (C) Fractionated cells (20 000; R3-R6) were cultured on OP9 cells. On day 7 of culture, hematopoietic clusters (red arrowheads) were developed only from the R3 fraction. In other fractions (R4-R6) hematopoietic clusters were not developed, but embryoid body–like colonies (blue arrowheads) developed from R5 and R6 fractions. Cells were analyzed at low (×40) magnification.

Development of hematopoietic, lymphatic endothelial, and blood vessel endothelial cells from Flk1$^+$Tie2$^+$ cells

To analyze the differentiating potential of ES-derived cells, we fractionated cells on day 5 of culture using Tie2 and Flk1 mAb as shown in Figure 1A (bottom panel, R1-R4). Expression profiling of transcription factors specific for hematopoietic or endothelial cells was undertaken by RT-PCR (Figure 1B). Expression levels of GATA-2, SCL, and AML-1 in the Tie2$^+$Flk1$^+$ fraction (R3) were 1.7-, 2.5-, and 1.7-fold higher than those in the Tie2$^-$Flk1$^+$ fraction (R4), respectively. In the Flk1$^-$ fraction (R5 and R6), expression levels of these genes were much lower compared with the Tie2$^-$Flk1$^+$ fraction (R4), suggesting that the Tie2$^+$Flk1$^+$ fraction may contain committed progenitors of hematopoietic and endothelial lineages. Cells (20 000) fractionated by Flk1 and Tie2 expression were cultured on OP9 cells (Figure 1C), and hematopoietic clusters formed only from the Tie2$^+$Flk1$^+$ fraction (R3) (Figure 1C, red arrowheads). Hematopoietic clusters were not detected in Flk1$^+$Tie2$^-$ (R4), Flk1$^-$Tie2$^+$ (R5), or Flk1$^-$Tie2$^-$ fractions (R6). The number of hematopoietic progenitors in each fraction was estimated by colony-forming assays in methylcellulose culture (Figure 2A-B). BECs were detected by staining with PECAM-1 mAb (Figure 2C). PECAM-1$^+$ endothelial cells were spindle shaped and took up an acetyl-LDL (Figure 2D). To detect LECs, we generated a mAb against LYVE-1 (ALY7), a receptor for extracellular matrix glycosaminoglycan. Using this mAb, we detected LYVE-1$^+$ cells on OP9 cells (Figure 2E). These cells also took up acetyl-LDL (Figure 2F), and 65% of them expressed Tie2 (Figure 2I). The lymphatic identity of these cells was further demonstrated by RT-PCR, using primers specific for LEC-enriched genes, namely, *Pdpn*, *VEGFR3*, and *Prox1* (Figure 2J). Furthermore, LYVE-1$^+$ cells coexpressed Prox-1 (Figure 2K). The presence of VEGFR-3 transcripts in these cultures provided the impetus for us to add the lymphatic growth factors, VEGF-C and VEGF-D. The addition of these factors resulted in a marked increase in the number of LYVE-1$^+$ cells (Figure 2L) and an increase in the size of monolayers (VEGF-C, Figure 2G; VEGF-D, Figure 2H). These findings suggest that LYVE-1$^+$ cells derived from ES cell differentiation cultures express many genes that are restricted to or enriched in LECs.

That Tie2 is required for these cell types is supported by the more than 10-fold increase in hematopoietic, blood vessel endothelial, and lymphatic endothelial colonies from Tie2$^+$Flk1$^+$ cells compared with Tie2$^-$Flk1$^+$ or Tie2$^-$Flk1$^-$ cell fractions (Table 1). To determine which cells produce the Tie2 ligands Ang1, Ang2, and Ang3 in order to support Tie2$^+$ cells, we performed quantitative expression analysis for Ang1, Ang2, and Ang3. As shown in Figure 2M, OP9 cells and LYVE-1$^-$ ES-derived cells expressed Ang1 but not Ang2 or Ang3. Although low expression levels of

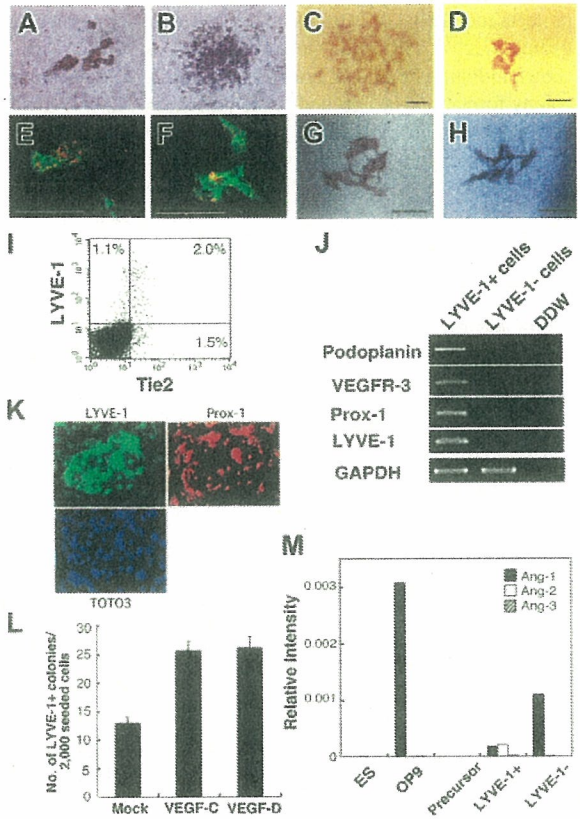

Figure 2. Development of lymphatic endothelial cells from ES cells. The Tie2$^+$Flk1$^+$ fraction of ES cell–derived cells formed erythroid colonies (A) and granulocyte-macrophage colonies (B) in methylcellulose. Vascular and lymphatic endothelial cells were stained with PECAM-1 mAb (C) and LYVE-1 mAb (D), respectively. PECAM-1$^+$ cells (green, panel E) and LYVE-1$^+$ cells (green, panel F) took up acetyl-LDL (red, panels E and F). Scale bars, 10 μm. (I) Expression of LYVE-1 and Tie2 in differentiated cells derived from ES cells on OP9 cells on day 6 of culture was analyzed by flow cytometry. The percentages of cells in each quadrant are indicated. (J) Lymphatic-specific genes, *Pdpn*, VEGFR-3, and Prox-1 in LYVE-1$^+$ and LYVE-1$^-$ cells were analyzed by RT-PCR. (K) Immunostaining at high magnification (× 200) showed that LYVE-1$^+$ cells (green) coexpressed Prox-1 (red). TOTO3 (blue) was used to stain nuclei. (L) In the presence of VEGF-C and VEGF-D (100 ng/mL each), the number of LYVE-1$^+$ colonies increased to 2 times that of mock-treated cells. Colonies were also larger in the presence of VEGF-C and VEGF-D (panels G and H, respectively). Results are expressed as the mean ± SD. (M) OP9 and ES cell–derived LYVE-1$^-$ cells expressed Ang1. LYVE-1$^+$ cells expressed low levels of Ang1 and Ang2. Ang1, Ang2, and Ang3 were not detectable in ES cells and lymphatic precursors (Flk1$^+$ cells derived from ES cells).

Ang1 and Ang2 were detected in LYVE-1$^+$ cells. ES cells and lymphatic precursor cells (ES cell–derived Flk1$^+$ cells) did not express Ang's. These results suggest that Ang1 derived from OP9 cells might affect the growth or survival of Tie2$^+$ cells.

Table 1. Frequency of hematopoietic and endothelial progenitors of differentiated ES cells

	Erythroid colonies from 30 000 cells	GM colonies from 30 000 cells	Vascular endothelial colonies from 1500 cells	Lymphatic endothelial colonies from 2000 cells
Tie2$^+$Flk1$^+$	11.3 ± 6.4	11.7 ± 2.1	47.5 ± 5.3	24.3 ± 2.5
Tie2$^-$Flk1$^+$	0	0	5.2 ± 1.8	0
Tie2$^+$Flk1$^-$	0	0	0	0
Tie2$^-$Flk1$^-$	0	0	0	0
Bulk	0	0	2.7 ± 1.5	1.3 ± 0.6

Development of hematopoietic and endothelial cells from Tie2-deficient ES cells

To clarify the function of Tie2 during hematopoietic and endothelial differentiation from ES cells, the differentiation capacity of *Tie2*$^{-/-}$ ES cells was examined using our culture system. *Tie2*$^{-/-}$ ES cells grew normally on MEF feeder layer cells (data not shown), and differentiated cells grown on OP9 cells were analyzed by flow cytometry. The frequency of cells expressing Flk1 in the *Tie2*$^{-/-}$ ES cells was similar to that seen in *Tie2*$^{+/-}$ cells (Figure 3A). RT-PCR of RNA from this fraction for expression of the genes involved in development of hematopoietic and endothelial cells revealed no remarkable differences between *Tie2*$^{+/-}$ and *Tie2*$^{-/-}$ cells (Figure 3B). To analyze hematopoietic development of *Tie2*$^{-/-}$ ES cells, we calculated the number of hematopoietic clusters formed on OP9 cells at day 7 of culture. The number and size of hematopoietic clusters of *Tie2*$^{-/-}$ ES cells were the same as those of *Tie2*$^{+/-}$ cells (Figure 3C, and data not shown). When the *Tie2*$^{-/-}$ hematopoietic clusters were transferred to fresh OP9 cells for an additional week, normal proliferating hematopoietic cells were detected by flow cytometry. Mature Mac-1–, Gr-1–, and Ter119–positive hematopoietic cells were differentiated from *Tie2*$^{-/-}$ ES cells (Figure 3D), and the frequency of mature hematopoietic cells was similar to that seen in *Tie2*$^{+/-}$ cells (data not shown), suggesting that Tie2 is not essential for development of hematopoietic cells. By contrast, *Tie2*$^{-/-}$ ES cells were severely defective in forming blood vessel and lymphatic endothelial colonies on OP9 cells at day 6 of culture. The number of such blood vessel and lymphatic endothelial colonies was approximately one

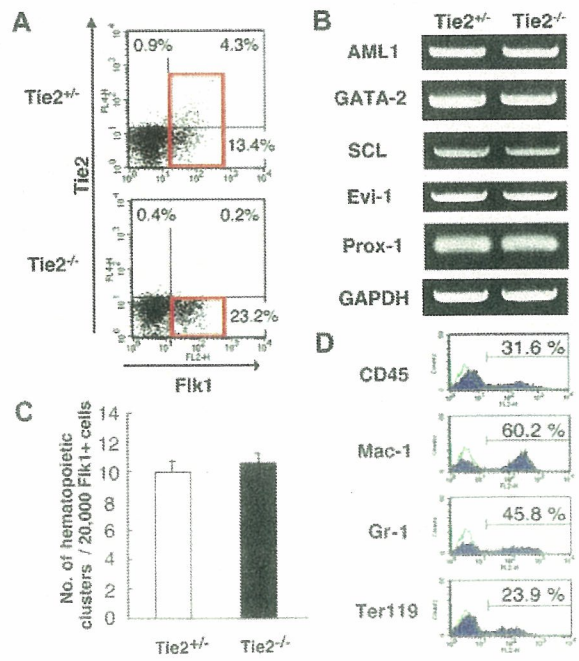

Figure 3. Normal development of hematopoietic cells from *Tie2*$^{-/-}$ ES cells. (A) FACS analysis of the expression of Flk1 and *Tie2* in *Tie2*$^{-/-}$ and *Tie2*$^{+/-}$ ES cell–differentiated cells. Red squares show the Flk1$^+$ fraction. The percentages of cells in each quadrant are indicated. (B) Expression of genes associated with mesoderm in Flk1$^+$ cells shown in panel A (red squares) was analyzed by RT-PCR. (C) Flk1$^+$ cells (20 000) were cultured on OP9 cells. The number of hematopoietic clusters from *Tie2*$^{+/-}$ and *Tie2*$^{-/-}$ cells at day 7 of culture was calculated. Results are expressed as the mean ± SD. (D) *Tie2*$^{-/-}$ hematopoietic clusters were cultured for an additional 7 days on fresh OP9 cells. The expression of CD45, Mac-1, Gr-1, and Ter119 was analyzed by flow cytometry. ES cell–derived hematopoietic cells are represented by purple shaded histograms; unstained controls, by green lines.

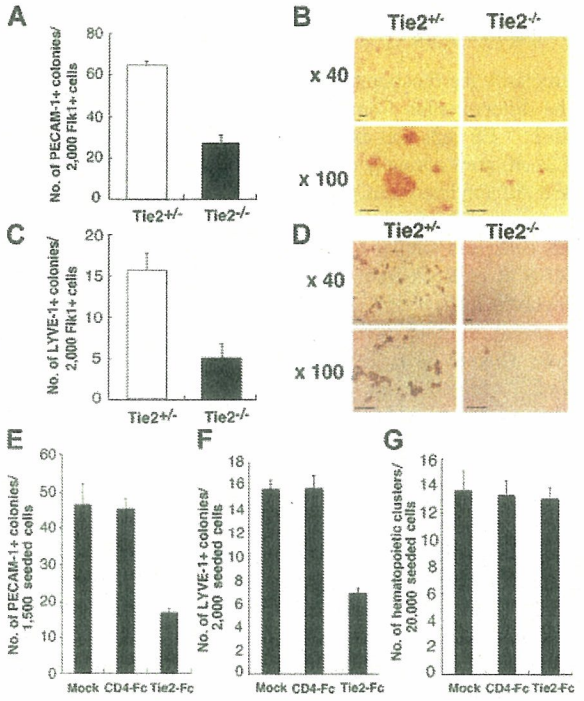

Figure 4. Lymphatic and blood vessel endothelial cell development from *Tie2*$^{-/-}$ ES cells. (A) Flk1^{+} cells (2000) were cultured on OP9 cells. At day 7 of culture, the number of vascular endothelial colonies developed from *Tie2*$^{+/-}$ (□) and *Tie2*$^{-/-}$ (■) ES cells was calculated. (B) Vascular endothelial colonies were stained with PECAM-1 mAb and analyzed at low (× 40) and high (× 100) magnification. (C) The number of lymphatic endothelial colonies developed from *Tie2*$^{+/-}$ (□) and *Tie2*$^{-/-}$ (■) ES cells was calculated. (D) Lymphatic endothelial colonies were stained with LYVE-1 mAb and analyzed at low (× 40) and high (× 100) magnification. Scale bars in panels B and D, 20 μm. In the presence of Tie2-Fc (30 μg/mL), the number of vascular and lymphatic endothelial colonies was decreased (panels E and F, respectively). (G) Hematopoietic cluster formation was not affected by exogenous soluble Tie2-Fc (30 μg/mL). Exogenous soluble CD4-Fc (30 μg/mL) served as the control. Results in panels A, C, and E-G are expressed as the mean ± SD.

third that observed from *Tie2*$^{+/-}$ cells (Figure 4A-B), and colony size was smaller than that seen from *Tie2*$^{+/-}$ cells (Figure 4C-D). These results suggest that Tie2 function is required for development of BECs and LECs, but not of hematopoietic cells. To confirm these findings, we added soluble Tie2-Fc fusion protein to the culture media of wild-type ES cells to block Tie2 signaling. As shown in Figure 4E-G, the number of vascular and lymphatic endothelial cell colonies derived from wild-type ES cells in the presence of soluble Tie2-Fc fusion protein decreased to one half to one third of the mock-treated cells, while the number of hematopoietic clusters was not affected by soluble Tie2-Fc fusion protein. We did not detect such inhibition in the presence of soluble CD4-Fc fusion protein (Figure 4 E-F).

Tie2 signaling is crucial for antiapoptotic signaling in the development of lymphatic and blood vessel endothelial cells

To further analyze the mechanisms underlying defective proliferation of BECs and LECs from *Tie2*$^{-/-}$ ES cells, we analyzed expression of blood vessel– and lymphatic-specific markers PECAM-1 and LYVE-1, respectively, by flow cytometry at days 2, 4, and 6 of culture (Figure 5A). Cells expressing PECAM-1 and LYVE-1 in *Tie2*$^{-/-}$ ES cells decreased over 6 days. PECAM-1^{+} cells in *Tie2*$^{-/-}$ cells were approximately one third the number of those in *Tie2*$^{+/-}$ cells at day 6 of culture, as was the case with LYVE-1^{+} cells (Figure 5B-C). This finding suggested that *Tie2*$^{-/-}$-mediated signaling protects endothelial cells from cell death. To test this possibility, we treated *Tie2*$^{-/-}$ cells with the caspase inhibitor Z-VAD-fmk. As shown in Figure 5B and C, lymphatic and blood vessel endothelial colony formation was rescued in the presence of Z-VAD-fmk in a dose-dependent fashion. In the presence of 50 nM of Z-VAD-fmk, the number of lymphatic endothelial colonies from *Tie2*$^{-/-}$ cells was rescued to 60% of that from *Tie2*$^{+/-}$ cells (Figure 5C), although the size of *Tie2*$^{-/-}$ lymphatic endothelial colonies remained small (Figure 5D). The formation of blood vessel endothelial colonies was similar in the presence of Z-VAD-fmk (50 nM; Figure 5C). These findings suggest that Tie2 signaling is crucial for LEC and BEC development and mediates antiapoptotic signaling during ES cell differentiation.

Discussion

Although we have demonstrated that Tie2 is expressed in the vitelline artery,[19] the AGM region,[4] and fetal liver,[20] the function of Tie2 in development has not been elucidated. The early death of Tie2$^{-/-}$ embryos precludes detailed analysis of the role of Tie2 in

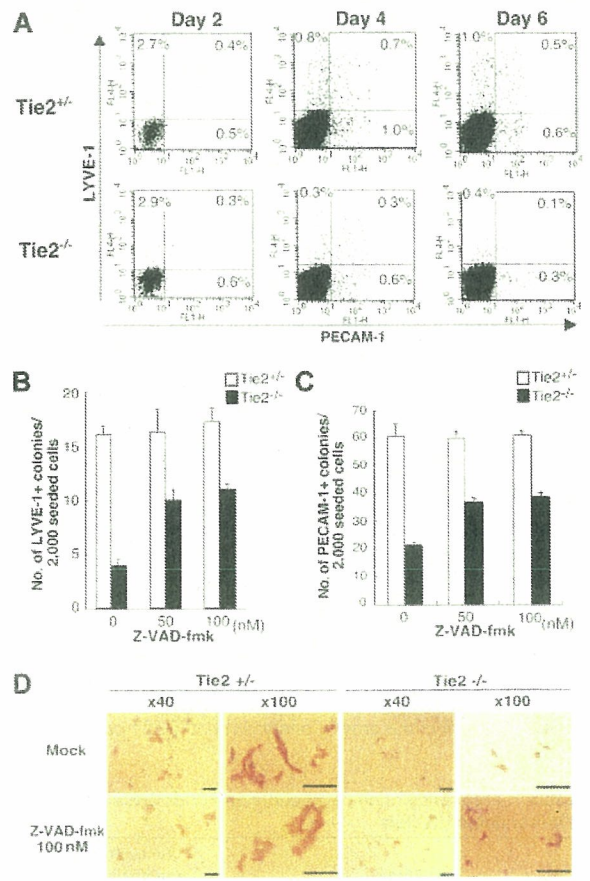

Figure 5. Tie2 signaling in blood vessels and lymphatic endothelial cells protected from apoptosis. (A) Expression of PECAM-1 and LYVE-1 in ES cell–derived cells was analyzed by flow cytometry at days 2, 4, and 6 of culture. The percentages of cells in each quadrant are indicated. (B) Addition of the caspase inhibitor Z-VAD-fmk (50 nM) to the culture media rescued the number of LYVE-1^{+} colonies from *Tie2*$^{-/-}$ ES cells (■). (C) The number of PECAM-1^{+} colonies from *Tie2*$^{-/-}$ ES cells (■) was also rescued in the presence of Z-VAD-fmk (50 nM). Results are expressed as mean ± SD. (D) In the presence of Z-VAD-fmk, the size of *Tie2*$^{-/-}$ lymphatic endothelial cells was unchanged, although the number of lymphatic colonies was partially rescued. Scale bars, 20 μm.

development of hematopoietic and endothelial lineages. Using an ES cell differentiation system, we have analyzed the development of hematopoietic cells as well as BECs and LECs from *Tie2*$^{-/-}$ ES cells. At day 8 of culture on OP9 cells, the normal formation of hematopoietic clusters from *Tie2*$^{-/-}$ cells suggests that Tie2 signaling does not contribute to development of hematopoietic cells from precursors. Furthermore, differentiation of myeloid cells from *Tie2*$^{-/-}$ hematopoietic clusters was normal. These results indicate that Tie2 is not essential for development of hematopoietic cells from ES cells. Recently, Puri and Bernstein[21] used combined mosaic analysis to demonstrate that Tie receptors are not required for differentiation and proliferation of definitive hematopoietic lineages in the embryo and fetus. Their findings are consistent with what we show in this study. Although our in vitro differentiation experiments suggest that Tie2 is not essential for hematopoiesis during development, Ang1/Tie2 signaling in hematopoietic cells has been reported to function to maintain hematopoietic stem cells in the bone marrow niche where Ang1 is expressed by osteoblasts.[18] Thus Tie2 function in hematopoiesis would seem to be specific for adult bone marrow.

Although much is known about normal and pathologic development of the vascular system,[35] the lack of specific markers has made it difficult to follow the development of the lymphatic system. In order to identify LECs, we recently generated a LEC-specific mAb against LYVE-1.[26] This mAb allowed us to detect LECs in mouse embryos at midgestation and purify these cells. ES cell–derived LYVE-1$^+$ cells express LEC-specific genes, such as *Prox1*, *Pdpn*, and *VEGFR3*, and exhibit DiI-Ac-LDL uptake. Furthermore, VEGF-C and VEGF-D, lymphatic growth factors, increased the number of LYVE-1–positive endothelial colonies from ES cells. These findings indicate that LYVE-1$^+$ cells isolated from these cultures have many characteristics of LECs. Lymphatic vasculature of the thoracic and abdominal viscera have been proposed to arise by endothelial spreading from lymph sacs.[6,36] This proposal is supported by the finding that budding of endothelial cells from the veins of Prox-1 mutant embryos is arrested.[9,10] To clarify the mechanisms of lymphangiogenesis in vitro, we analyzed the function of Tie2. In this study LECs were differentiated from ES cell–derived Tie2$^+$Flk1$^+$ cells, and approximately 1% of Tie2$^+$Flk1$^+$ cells formed lymphatic endothelial colonies on OP9 cells. Our in vitro differentiation assay allows us to clarify the mechanisms of LEC development from its precursor.

Thus far, Tie2 signaling has been reported to be required for proper development and function of the vascular system. Mice lacking Ang2 exhibit lymphatic vessel defects, strongly suggesting a role of Tie2 signaling in lymphangiogenesis.[37] In this study we have shown that LECs and BECs can be differentiated from Tie2$^+$Flk1$^+$ cells, and that 65% of LYVE-1$^+$ LECs express Tie2. To analyze the function of Tie2 in the development of lymphatic endothelial cells, we performed FACS analysis and immunocytochemistry during differentiation of *Tie2*$^{-/-}$ ES cells. FACS analysis revealed that *Tie2*$^{-/-}$ cells expressing LYVE-1 decreased over time as did PECAM-1$^+$ BECs. Treatment with a caspase inhibitor, which specifically inhibits apoptosis, partially rescued defective formation of lymphatic and blood vessel endothelial colonies from *Tie2*$^{-/-}$ cells, suggesting that both endothelial cells undergo apoptosis in the absence of Tie2 signaling. Although Tie2 signaling contributed to the survival of both LECs and BECs on OP9 cells, treatment with the caspase inhibitor did not affect the size of *Tie2*$^{-/-}$ colonies. Based on these findings, we propose that Tie2 cooperates with other signaling pathways involved in growth. Although we do not identify these pathways, OP9 cells are known to secrete several growth factors, including VEGF-C and VEGF-D.[38] FACS analysis also revealed that at day 2 of culture, the frequency of LYVE-1$^+$ and PECAM-1$^+$ cells derived from *Tie2*$^{-/-}$ cells was comparable with frequencies seen in *Tie2*$^{+/-}$ cells, suggesting that lymphatic and blood vessel endothelial precursors develop normally from *Tie2*$^{-/-}$ cells. A gene expression study clearly showed that expression levels of Prox-1 in lymphatic precursors (the Flk1$^+$ cell fraction) of *Tie2*$^{-/-}$ cells were comparable with those seen in *Tie2*$^{+/-}$ cells, suggesting that Tie2 deficiency does not affect Prox-1 expression. These findings suggest that Tie2 is not essential for development of lymphatic and blood vessel endothelial precursors, although both types of endothelial cells from *Tie2*$^{-/-}$ cells undergo apoptosis due to lack of Tie2 signaling.

Regarding vascular endothelial cells, in vivo study has shown that mice lacking Ang1 and Tie2 develop a fairly normal primary vasculature, but that this vasculature fails to undergo further normal remodeling.[28,39,40] We have demonstrated that lymphatic endothelial cells express Tie2 in both embryonic and adult settings, and that the activation of Tie2 signaling by Ang1 stimulates both in vivo lymphatic angiogenesis in mouse cornea and in vitro colony formation of lymphatic endothelial cells.[26] Data from both in vitro ES cell differentiation and in vivo embryonic development suggest that Ang/Tie2 signaling may contribute to regulation of lymphatic vessel formation in the development of lymphatic vessels.

In summary, our results derived from induction studies of ES cells have revealed that Tie2 is expressed in the precursors of mesodermal lineages, hematopoietic cells, and endothelial cells. We have also shown that Tie2 is not essential for development of hematopoietic cells, but that it plays an important role in antiapoptotic signaling in lymphatic and blood vessel development.

Acknowledgment

We thank Ms Ayami Ono for expert assistance in the FACS analysis.

References

1. Sabin F. Studies on the origin of blood vessels and red corpuscles as seen in the living blastoderm of the chick during the second day of incubation. Contribut Embryol. 1920;9:213-262.
2. Kubo H, Alitalo K. The bloody fate of endothelial stem cells. Genes Dev. 2003;17:322-329.
3. Haar JL, Ackerman GA. A phase and electron microscopic study of vasculogenesis and erythropoiesis in the yolk sac of the mouse. Anat Rec. 1971;170:199-223.
4. Hamaguchi I, Huang XL, Takakura N, et al In vitro hematopoietic and endothelial cell development from cells expressing TEK receptor in murine aorta-gonad-mesonephros region. Blood. 1999; 93:1549-1556.
5. Choi K, Kennedy M, Kazarov A, Papadimitriou JC, Keller G. A common precursor for hematopoietic and endothelial cells. Development. 1998; 125:725-732.
6. Sabin FR. On the origin of the lymphatic system from the veins, and the development of the lymph hearts and thoracic duct in the pig. Am J Anat. 1902;1:367-389.
7. Oliver G, Detmar M. The rediscovery of the lymphatic system: old and new insights into the development and biological function of the lymphatic vasculature. Genes Dev. 2002;16:773-783.
8. Jeltsch M, Kaipainen A, Joukov V, et al. Hyperplasia of lymphatic vessels in VEGF-C transgenic mice. Science. 1997;276:1423-1425.
9. Wigle JT, Oliver G. Prox1 function is required for the development of the murine lymphatic system. Cell. 1999;98:769-778.
10. Wigle JT, Harvey N, Detmar M, et al. An essential role for Prox1 in the induction of the lymphatic endothelial cell phenotype. EMBO J. 2002;21: 1505-1513.
11. Shalaby F, Rossant J, Yamaguchi TP, et al. Failure of blood-island formation and vasculogenesis in Flk-1-deficient mice. Nature. 1995;376:62-66.

12. Shalaby F, Ho J, Stanford WL, et al. A requirement for Flk1 in primitive and definitive hematopoiesis and vasculogenesis. Cell. 1997;89:981-990.
13. Millauer B, Wizigmann-Voos S, Schnurch H, et al. High affinity VEGF binding and developmental expression suggest Flk-1 as a major regulator of vasculogenesis and angiogenesis. Cell. 1993;72: 835-846.
14. Dumont DJ, Fong GH, Puri MC, Gradwohl G, Alitalo K, Breitman ML. Vascularization of the mouse embryo: a study of flk-1, tek, tie, and vascular endothelial growth factor expression during development. Dev Dyn. 1995;203:80-92.
15. de Vries C, Escobedo JA, Ueno H, Houck K, Ferrara N, Williams LT. The fms-like tyrosine kinase, a receptor for vascular endothelial growth factor. Science. 1992;255:989-991.
16. Dumont DJ, Gradwohl GJ, Fong GH, Auerbach R, Breitman ML. The endothelial-specific receptor tyrosine kinase, tek, is a member of a new subfamily of receptors. Oncogene. 1993;8:1293-1301.
17. Iwama A, Hamaguchi I, Hashiyama M, Murayama Y, Yasunaga K, Suda T. Molecular cloning and characterization of mouse TIE and TEK receptor tyrosine kinase genes and their expression in hematopoietic stem cells. Biochem Biophys Res Commun. 1993;195:301-309.
18. Arai F, Hirao A, Ohmura M, et al. Tie2/angiopoietin-1 signaling regulates hematopoietic stem cell quiescence in the bone marrow niche. Cell. 2004; 118:149-161.
19. Takakura N, Huang XL, Naruse T, et al. Critical role of the TIE2 endothelial cell receptor in the development of definitive hematopoiesis. Immunity. 1998;9:677-686.
20. Hsu HC, Ema H, Osawa M, Nakamura Y, Suda T, Nakauchi H. Hematopoietic stem cells express Tie-2 receptor in the murine fetal liver. Blood. 2000;96:3757-3762.
21. Puri MC, Bernstein A. Requirement for the TIE family of receptor tyrosine kinases in adult but not fetal hematopoiesis. Proc Natl Acad Sci U S A. 2003;100:12753-12758.
22. Koblizek TI, Weiss C, Yancopoulos GD, Deutsch U, Risau W. Angiopoietin-1 induces sprouting angiogenesis in vitro. Curr Biol. 1998;8:529-532.
23. Papapetropoulos A, Garcia-Cardena G, Dengler TJ, Maisonpierre PC, Yancopoulos GD, Sessa WC. Direct actions of angiopoietin-1 on human endothelium: evidence for network stabilization, cell survival, and interaction with other angiogenic growth factors. Lab Invest. 1999;79:213-223.
24. Kwak HJ, So JN, Lee SJ, Kim I, Koh GY. Angiopoietin-1 is an apoptosis survival factor for endothelial cells. FEBS Lett. 1999;448:249-253.
25. Jones N, Voskas D, Master Z, Sarao R, Jones J, Dumont DJ. Rescue of the early vascular defects in Tek/Tie2 null mice reveals an essential survival function. EMBO Rep. 2001;2:438-445.
26. Morisada T, Oike Y, Yamada Y, et al. Angiopoietin-1 promotes LYVE-1-positive lymphatic vessel formation. Blood. 2005;105:4649-4656.
27. Tammela T, Saaristo A, Lohela M, et al. Angiopoietin-1 promotes lymphatic sprouting and hyperplasia. Blood. 2005;105:4624-4648.
28. Dumont DJ, Gradwohl G, Fong GH, et al Dominant-negative and targeted null mutations in the endothelial receptor tyrosine kinase, tek, reveal a critical role in vasculogenesis of the embryo. Genes Dev. 1994;8:1897-1909.
29. Puri MC, Rossant J, Alitalo K, Bernstein A, Partanen J. The receptor tyrosine kinase TIE is required for integrity and survival of vascular endothelial cells. EMBO J. 1995;14:5884-5891.
30. Yagi T, Tokunaga T, Furuta Y, et al. A novel ES cell line, TT2, with high germline-differentiating potency. Anal Biochem. 1993;214:70-76.
31. Hooper M, Hardy K, Handyside A, Hunter S, Monk M. HPRT-deficient (Lesch-Nyhan) mouse embryos derived from germline colonization by cultured cells. Nature. 1987;326:292-295.
32. Nagy A, Rossant J, Nagy R, Abramow-Newerly W, Roder JC. Derivation of completely cell culture-derived mice from early-passage embryonic stem cells. Proc Natl Acad Sci U S A. 1993;90: 8424-8428.
33. Takakura N, Yoshida H, Ogura Y, Kataoka H, Nishikawa S. PDGFR alpha expression during mouse embryogenesis: immunolocalization analyzed by whole-mount immunohistostaining using the monoclonal anti-mouse PDGFR alpha antibody APA5. J Histochem Cytochem. 1997;45: 883-893.
34. Yano M, Iwama A, Nishio H, Suda J, Takada G, Suda T. Expression and function of murine receptor tyrosine kinases, TIE and TEK, in hematopoietic stem cells. Blood. 1997;89:4317-4326.
35. Gale NW, Yancopoulos GD. Growth factors acting via endothelial cell-specific receptor tyrosine kinases: VEGFs, angiopoietins, and ephrins in vascular development. Genes Dev. 1999;13:1055-1066.
36. Gray H. In Anatomy of the human body. In: Clemente CD, ed. The Lymphatic System. Philadelphia, PA: Lea and Febiger; 1985:866-932.
37. Gale NW, Thurston G, Hackett SF, et al. Angiopoietin-2 is required for postnatal angiogenesis and lymphatic patterning, and only the latter role is rescued by Angiopoietin-1. Dev Cell. 2002;3: 411-423.
38. Matsumura K, Hirashima M, Ogawa M, et al. Modulation of VEGFR-2-mediated endothelial-cell activity by VEGF-C/VEGFR-3. Blood. 2003; 101:1367-1374.
39. Suri C, Jones PF, Patan S, et al. Requisite role of angiopoietin-1, a ligand for the TIE2 receptor, during embryonic angiogenesis. Cell. 1996;87:1171-1180.
40. Sato TN, Tozawa Y, Deutsch U, et al. Distinct roles of the receptor tyrosine kinases Tie-1 and Tie-2 in blood vessel formation. Nature. 1995; 376:70-74.

Available online at www.sciencedirect.com
SCIENCE DIRECT
ELSEVIER
Leukemia Research 30 (2006) 90–97
Leukemia Research
www.elsevier.com/locate/leukres

Open forum

In vitro and in vivo antitumor activity of the NF-κB inhibitor DHMEQ in the human T-cell leukemia virus type I-infected cell line, HUT-102

Takeo Ohsugi [a,*], Toshio Kumasaka [b], Akira Ishida [c], Takaomi Ishida [d], Ryouichi Horie [e], Toshiki Watanabe [d], Kazuo Umezawa [f], Kazunari Yamaguchi [g]

[a] *Division of Microbiology and Genetics, Center for Animal Resources and Development, Institute of Resource Development and Analysis, Kumamoto University, 2-2-1 Honjo, Kumamoto 860-0811, Japan*
[b] *Department of Pathology (I), Juntendo University School of Medicine, 2-1-1 Hongo, Bunkyo-ku, Tokyo 113-8421, Japan*
[c] *Department of Computer and Media Science, Faculty of Engineering, Yamanashi University, 4-3-11 Takeda, Kofu 400-8510, Japan*
[d] *Division of Pathology, Department of Cancer Research, The Institute of Medical Science, The University of Tokyo, 4-6-1 Shirokanedai, Minato-ku, Tokyo 108-8639, Japan*
[e] *Department of Hematology, Faculty of Medicine, Kitasato University, 1-15-1 Sagamihara, Kanagawa 228-8555, Japan*
[f] *Department of Applied Chemistry, Faculty of Science and Technology, Keio University, 3-14-1 Hiyoshi, Kohoku-ku, Yokohama 223-0061, Japan*
[g] *Department of Safety Research on Blood and Biologics, National Institute of Infectious Diseases, Gakuen 4-7-1, Musashimurayama-shi, Tokyo 208-0011, Japan*

Received 24 December 2004; accepted 31 May 2005
Available online 5 July 2005

Abstract

Adult T-cell leukemia (ATL) is an aggressive neoplasm caused by human T-cell leukemia virus type I (HTLV-I). The NF-κB pathway is activated in ATL cells and in virus-infected cells, and plays a central role in oncogenesis. We examined the effect of the novel NF-κB inhibitor, dehydroxymethylepoxyquinomicin (DHMEQ), on a well-characterized HTLV-I-infected cell line, HUT-102, in vitro and in vivo. DHMEQ inhibited translocation of NF-κB p65 to the nucleus and induced apoptotic cell death in vitro. In vivo, DHMEQ inhibited the growth and infiltration of HUT-102 tumor cells transplanted subcutaneously in SCID mice lacking natural killer cell activity.

Keywords: Animal model; ATL; DHMEQ; HTLV-I; NF-κB; NF-κB inhibitor; Mice

1. Introduction

Adult T-cell leukemia (ATL) is a peripheral CD4-positive T-cell neoplasm caused by human T-cell leukemia virus type I (HTLV-I) infection [1,2]. ATL is an aggressive and lethal disease for which there is no effective treatment. It was recently reported that the nuclear transcription factor, NF-κB, plays a central role in oncogenesis induced by HTLV-I [3] and that NF-κB activity is required for ATL cell survival [4].

In resting T-cells, NF-κB is sequestered in the cytoplasm as a latent precursor by its inhibitor, IκBα. Subsequent to cellular activation and through proteolytic degradation of IκBα, NF-κB is released and translocates to the nucleus where it transactivates various genes encoding cytokines, chemokines and antiapoptotic proteins. HTLV-I-encoded Tax binds to IKKγ/NEMO, resulting in enhanced degradation of IκBα and activation of NF-κB in HTLV-I-infected cells [5,6]. On the other hand, ATL cells lacking Tax expression also utilize the activated NF-κB pathway [7] through an unknown mechanism. Furthermore, we recently reported that NF-κB is constitutively activated in untransformed HTLV-I-infected cells in the peripheral blood of virus carriers [8]. Thus, constitutive activation of NF-κB appears to be a molecular mechanism

Abbreviations: ATL, adult T-cell leukaemia; DHMEQ, dehydroxymethylepoxyquinomicin; HTLV-I, human T-cell leukemia virus type

* Corresponding author. Tel.: +81 96 373 6549; fax: +81 96 373 6552.
E-mail address: ohsugi@gpo.kumamoto-u.ac.jp (T. Ohsugi).

0145-2126/$ – see front matter © 2005 Elsevier Ltd. All rights reserved.
doi:10.1016/j.leukres.2005.06.001

that drives aberrant growth and cytokine gene expression in ATL cells, thereby making it an ideal target for developing molecular therapeutics for ATL.

We have developed a novel NF-κB inhibitor, dehydroxymethylepoxyquinomicin (DHMEQ) [9]. DHMEQ is a 5-dehydroxymethyl derivative of epoxyquinomicin C, an antibiotic originally isolated from *Amicolatopsis* sp. [10]. Most NF-κB inhibitors inhibit IκBα phosphorylation, whereas DHMEQ inhibits nuclear translocation of p65, a component of NF-κB [11]. DHMEQ is effective in treating a hormone-refractory prostate cancer model in nude mice [12], multiple myeloma both in vitro and in a SCID mouse model [13]. Also, DHMEQ strongly inhibits constitutively activated NF-κB in both ATL-derived cell lines and in freshly cultured primary ATL cells from patients, inducing apoptosis of these cells at concentrations that do not affect the viability of peripheral blood mononuclear cells [8]. DHMEQ has not shown toxicity in animals [9,11], suggesting that it is specific for NF-κB.

In this study, we used a well-characterized HTLV-I-infected cell line, HUT-102, to evaluate the antiproliferative activity of DHMEQ in vitro and in vivo. The results show that DHMEQ inhibits cell proliferation and induces apoptotic cell death in vitro and blocks tumor growth and infiltration of HUT-102 cells to various organs in vivo.

2. Materials and methods

2.1. Cell lines

The HTLV-I-infected T-cell line, HUT-102 [1], was maintained in RPMI 1640 supplemented with 10% fetal bovine serum (FBS), 100 U/ml of penicillin and 100 μg/ml of streptomycin at 37 °C in 5% CO_2. The HTLV-I-negative T-cell line, MOLT-4, was maintained in RPMI 1640 supplemented with 10% FBS and the above antibiotics. These cells lines were passaged twice a week.

2.2. Chemicals

Racemic DHMEQ was synthesized as described [9], dissolved in DMSO and subsequently diluted in culture medium to a final DMSO concentration of <0.1%.

2.3. NF-κB activity

HUT-102 cells (5×10^6) were cultured with 20 or 40 μg/ml DHMEQ for 16 h. Cells treated with DMSO solution lacking DHMEQ served as a control. The DNA-binding activity of NF-κB p65 was measured using an enzyme-linked immunosorbent assay (ELISA) according to the manufacturer's protocol (Trans-AM NF-κB p65 Transcription Factor Assay Kit; Active Motif North America, Carlsbad, CA). The absorbance in each well was determined at 450 nm using a microplate reader (Bio-Rad, Richmond, CA). NF-κB activity was determined as the DNA-binding of p65 and is expressed as a percentage of the binding measured in control cells that were not treated with DHMEQ.

2.4. Real-time quantitative reverse transcription-PCR (RT-PCR)

Total cellular RNA was prepared using the RNeasy Kit (Qiagen, Valencia, CA) as recommended by the manufacturer. Approximately 0.5 μg of total RNA was used in the RT reaction, which was performed at 25 °C for 10 min, at 48 °C for 30 min and then at 95 °C for 5 min using the TaqMan® Reverse Transcription Kit (Applied Biosystems, Foster City, CA). To measure HTLV-I Tax expression, real-time PCR was performed using an ABI-Prism 7700 Sequence Detector (Applied Biosystems). LUX™ primers were obtained from Invitrogen (Carlsbad, CA). The primers for the Tax region of HTLV-I were as follows: forward hairpin primer 5′-GTACATGGGCTCCGTTGTCTGCATGTAC-3′ labeled with 6-carboxy-fluorescein (FAM) (underlined T), reverse primer 5′-CGCTTGTAGGGAACATTGGTG-3′. Real-time PCR cycles started with 2 min at 50 °C, 2 min at 95 °C, and then 45 cycles of 15 s at 95 °C, 30 s at 55 °C and 30 s at 72 °C. Used as an internal control, human GAPDH was assessed using premixed reagents from Invitrogen. Detection of Tax and human GAPDH was performed using Platinum® Quantitative PCR SuperMix-UDG (Invitrogen).

2.5. Detection of NF-κB p50 and p65

Cells (2.5×10^6) in a 6-cm dish were cultured with 20 or 40 μg/ml DHMEQ for 16 h. Cells treated with DMSO solution lacking DHMEQ served as a control. Cells were washed twice with phosphate buffered saline (PBS), dried on a slide glass and fixed with 100% methanol for 10 min. After fixation, cells were washed three times with PBS. Samples were first incubated with a rabbit polyclonal antibody for NF-κB p50 or p65 (Abcam, Cambridge, UK) for 30 min at room temperature and then stained with FITC-conjugated anti-rabbit IgG (Jackson ImmunoResearch, West Grove, PA). Protein localization was detected using fluorescence microscopy (Olympus, Tokyo, Japan). MOLT-4 cells served as a control, using the same procedure.

2.6. Growth inhibition assay

The effect of DHMEQ on HUT-102 cell growth was assayed by the 3-(4,5-dimethylthiazol-2-yl)-5-(3-carboxymethoxyphenyl)-2-(4-sulfophenyl)-2H-tetrazolium, inner salt (MTS) method (CellTiter 96 Aqueous One Solution Cell Proliferation Assay; Promega, Madison, WI). Briefly, 5×10^4 cells were incubated in a 96-well microculture plate with various concentrations of DHMEQ. Cells treated with DMSO solution lacking DHMEQ served as a control. After 24 or 48 h of incubation, 20 μl of MTS solution was added, and the cells were incubated for another 2 h. The absorbance